

ARMY RESEARCH LABORATORY



Vibrational Mode Selectivity
in the Unimolecular
Decomposition of CH_2NNO_2

Betsy M. Rice

John Grosh

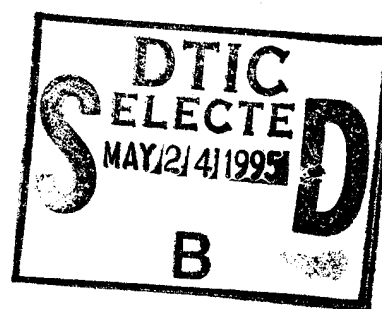
U.S. ARMY RESEARCH LABORATORY

Donald L. Thompson

OKLAHOMA STATE UNIVERSITY

ARL-TR-740

May 1995



APPROVED FOR PUBLIC RELEASE; DISTRIBUTION IS UNLIMITED.

19950522 068

DTIC QUALITY INSPECTED 1

NOTICES

Destroy this report when it is no longer needed. DO NOT return it to the originator.

Additional copies of this report may be obtained from the National Technical Information Service, U.S. Department of Commerce, 5285 Port Royal Road, Springfield, VA 22161.

The findings of this report are not to be construed as an official Department of the Army position, unless so designated by other authorized documents.

The use of trade names or manufacturers' names in this report does not constitute endorsement of any commercial product.

REPORT DOCUMENTATION PAGE

Form Approved
OMB No. 0704-0188

Public reporting burden for this collection of information is estimated to average 1 hour per response, including the time for reviewing instructions, searching existing data sources, gathering and maintaining the data needed, and completing and reviewing the collection of information. Send comments regarding this burden estimate or any other aspect of this collection of information, including suggestions for reducing this burden, to Washington Headquarters Services, Directorate for Information Operations and Reports, 1215 Jefferson Davis Highway, Suite 1204, Arlington, VA 22202-4302, and to the Office of Management and Budget, Paperwork Reduction Project (0704-0188), Washington, DC 20503.

1. AGENCY USE ONLY (Leave blank)		2. REPORT DATE May 1995	3. REPORT TYPE AND DATES COVERED Final, Sep 94-Jan 95	
4. TITLE AND SUBTITLE Vibrational Mode Selectivity in the Unimolecular Decomposition of CH ₂ NNO ₂			5. FUNDING NUMBERS PR: 1L161102AH43	
6. AUTHOR(S) Betsy M. Rice, John Grosh, and Donald L. Thompson*				
7. PERFORMING ORGANIZATION NAME(S) AND ADDRESS(ES) U.S. Army Research Laboratory ATTN: AMSRL-WT-PC Aberdeen Proving Ground, MD 21005-5066			8. PERFORMING ORGANIZATION REPORT NUMBER ARL-TR-740	
9. SPONSORING / MONITORING AGENCY NAME(S) AND ADDRESS(ES)			10. SPONSORING / MONITORING AGENCY REPORT NUMBER	
11. SUPPLEMENTARY NOTES *Donald L. Thompson is from the Department of Chemistry, Oklahoma State University, Stillwater, OK.				
12a. DISTRIBUTION / AVAILABILITY STATEMENT Approved for public release; distribution is unlimited.			12b. DISTRIBUTION CODE	
13. ABSTRACT (Maximum 200 words) Vibrational mode selectivity has been investigated for the unimolecular decomposition of methylene nitramine (MN), CH ₂ NNO ₂ , by using classical trajectories computed on a (previously reported) potential-energy surface (PES) that is based on ab initio results. The PES allows for the two known primary decomposition pathways: (I) N-N bond scission to form H ₂ CN and NO ₂ , and (II) concerted molecular elimination giving HONO and HCN. Rates were computed for 57.7 kcal/mol above the zero-point energy for initial conditions corresponding to overtone excitations of each of the 15 normal modes. One calculation was done at this energy with initial conditions corresponding to a microcanonical (statistical) distribution in which the energy was randomly distributed among all of the vibrational modes. Comparisons of the mode selective results with this statistical rate show that there is substantial enhancement of the decomposition rates for the two reactions for excitation of three of the normal modes. Excitation of the other 12 modes yielded rates in accord with the statistical rates for the two reactions. The results show that projection of a vibrational mode onto the reaction coordinate is necessary for mode selective reaction, but is not sufficient since energy transfer into the reaction coordinate must compete with energy flow to other modes that do not project onto (that is, are uncoupled from) the reaction coordinates.				
14. SUBJECT TERMS molecular dynamics, mode specific, unimolecular decomposition			15. NUMBER OF PAGES 41	
			16. PRICE CODE	
17. SECURITY CLASSIFICATION OF REPORT UNCLASSIFIED	18. SECURITY CLASSIFICATION OF THIS PAGE UNCLASSIFIED	19. SECURITY CLASSIFICATION OF ABSTRACT UNCLASSIFIED	20. LIMITATION OF ABSTRACT UL	

INTENTIONALLY LEFT BLANK.

ACKNOWLEDGMENTS

Mr. Donald L. Thompson gratefully acknowledges support from the U.S. Army Research Office. Some of the calculations were performed at the Department of Defense (DOD) High-Performance Computing Center (HPC) at the Corps of Engineers Waterways Experimental Station (CEWES), Vicksburg, MS.

Accession For	
NTIS GRA&I	<input checked="" type="checkbox"/>
DTIC TAB	<input type="checkbox"/>
Unannounced	<input type="checkbox"/>
Justification	
By	
Distribution/	
Availability Codes	
Dist	Avail and/or Special
A-1	

INTENTIONALLY LEFT BLANK.

TABLE OF CONTENTS

	<u>Page</u>
ACKNOWLEDGMENTS	iii
LIST OF FIGURES	vii
LIST OF TABLES	ix
1. INTRODUCTION	1
2. POTENTIAL ENERGY SURFACE	3
3. METHODS	3
4. RESULTS AND DISCUSSION	7
5. SUMMARY	24
6. REFERENCES	29
DISTRIBUTION LIST	31

INTENTIONALLY LEFT BLANK.

LIST OF FIGURES

<u>Figure</u>	<u>Page</u>
1. Depiction of the normal modes of vibration of equilibrium CH_2NNO_2 predicted by Mowrey et al. (1990)	4
2. Depiction of the normal modes of vibration of equilibrium CH_2NNO_2 predicted by the analytic PES used in this study and in Zhao, Hints, and Lee 1988	5
3. Decay curves for (a) Reference set (statistical initial conditions); (b) Mode 101; (c) Mode 275; (d) Mode 442; (e) Mode 560; (f) Mode 606; (g) Mode 753; (h) Mode 894; (i) Mode 1246; (j) Mode 1263, (k) Mode 1323; (l) Mode 1454; (m) Mode 1613; (n) Mode 1843; (o) Mode 3363; and (p) Mode 3489	8
4. Branching ratios for (a) Mode 101; (b) Mode 560; (c) Mode 606; (d) Mode 894; (e) Mode 1246; (f) Mode 1263; (g) Mode 1323; (h) Mode 1454; (i) Mode 1613; (j) Mode 1843; (k) Mode 3363; and (l) Mode 3489. These linear plots correspond to the linear decay curves shown in Figure 5	10
5. Branching ratios for (a) Reference set; (b) Mode 275; (c) Mode 442; and (d) Mode 753	11
6. Comparison of (a) k_{Total} , (b) k_1 , and (c) k_2 as a function of initial condition selection	12
7. Potential energy along the reaction path for Reaction [1]	15
8. Potential energy along the reaction path for Reaction [2]	16
9. Projection of the eigenvectors of the normal modes of CH_2NNO_2 (at equilibrium) onto the unit vector that points along the reaction path for (a) Reaction [1] and (b) Reaction [2]	18
10. Normal mode energy vs. time averaged over 50 trajectories for which 57.7 kcal/mol was initially placed in Mode 275	19
11. Normal mode energy vs. time averaged over 50 trajectories for which 57.7 kcal/mol was initially placed in Mode 442	20
12. Normal mode energy vs. time averaged over 50 trajectories for which 57.7 kcal/mol was initially placed in Mode 753	21
13. Normal mode energy vs. time averaged over 50 trajectories for which 57.7 kcal/mol was initially placed in Mode 606	22

<u>Figure</u>		<u>Page</u>
14.	Decay curve for trajectory ensemble in which 57.7 kcal/mol above the zero-point energy is equally partitioned to Modes 275 and 442	25
15.	Branching ratios corresponding to the decay curve shown in Figure 14	26

LIST OF TABLES

<u>Table</u>		<u>Page</u>
1.	End Tests	7
2.	Decay Coefficients and Branching Ratios	13
3.	Ensemble Results: Primary Decomposition Reactions	14

INTENTIONALLY LEFT BLANK.

1. INTRODUCTION

We report here a classical trajectory study of mode specificity in the unimolecular decomposition of CH_2NNO_2 . Methylene nitramine, CH_2NNO_2 , is believed to be the primary decomposition product of hexahydro-1,3,5-trinitro-1,3,5-triazine, more commonly referred to as RDX (Zhao, Hintsä, and Lee 1988). CH_2NNO_2 has never been isolated, but appears to decompose spontaneously to form simple di- and triatomic products (Zhao, Hintsä, and Lee 1988). The experimental results show that of two possible primary decomposition reactions,



CH_2NNO_2 decomposes only through concerted reaction (Zhao, Hintsä, and Lee 1988).

Classical trajectories (Rice et al., to be published), integrated under microcanonical conditions in which sufficient energy for reaction was partitioned statistically among the internal modes of the molecule, indicate that Reaction [1] is more probable, in direct contradiction to the experimental observation. This observation raised several questions, some of which are reviewed and addressed here.

Mowrey et al. (1990) suggested that either (a) Reaction [1] has an anomalous behavior in the rate, which makes this reaction improbable, or (b) Reaction [2] has a substantially lower activation energy than Reaction [1]. They investigated the latter case by performing multiconfigurational (MC) SCF and multireference (MR) CI calculations at critical points along the reaction paths for Reactions [1] and [2]. They estimated that the activation energy of Reaction [2], 31 ± 4 kcal/mol, is lower than, or at least comparable (within the error of their calculations) to the dissociation energy of the N-N bond (35 ± 4 kcal/mol).

We investigated the possibility of anomalous behavior of the reaction rates in a classical trajectory study of the unimolecular decomposition of CH_2NNO_2 (Rice et al., to be published). We developed a potential energy surface (PES) based on the Mowrey et al. (1990) results that reproduced the properties of the reactant, transition state leading to Reaction [2], and the products of both reactions. Structures, the corresponding energies and energy second derivatives at critical points and reaction path points predicted

by the ab initio calculations (Mowrey et al. 1990) were used to parameterize the analytic PES (Rice et al., to be published). Additionally, we incorporated experimental data for the products, where available, in our model. We integrated classical trajectories over the energy range 61 to 121 kcal/mol (including the zero-point energy), with the energy partitioned statistically among the internal modes via Metropolis Monte Carlo sampling (Metropolis et al. 1953; Raff and Thompson 1985). The results indicate that at all energies, Reaction [1] is most probable, but with Reaction [2] becoming increasingly important at higher energies. The rate coefficients are well-behaved with increasing energy and can be accurately fitted by the statistical RRK model of unimolecular reactions (Robinson and Holbrook 1972). The results of this study answered one of the questions raised by Mowrey et al. (1990): The rate constant for Reaction [1] has no anomalous behavior with increasing energy. Additionally, the dynamics calculations indicate that Reaction [1] is favored, except at the limit of high energy.

The results of the previous trajectory study (Rice et al., to be published) indicate that a more thorough understanding of the reaction dynamics of this molecule are needed to augment the conclusions of the experimental study (Rice et al., to be published). If the system has no anomalous behavior in the decay rates, and if the energetics of the reaction channels are correctly described in the model, why was Reaction [1] not observed in the experiment (Zhao, Hintsa, and Lee 1988)? In the present study, we investigate the possibility that upon formation of CH_2NNO_2 through the decomposition of RDX, energy is either placed directly into the reaction coordinate leading to Reaction [2] or into internal modes that are strongly coupled to that reaction coordinate.

Our investigation into this possibility is of interest not only for this specific chemical system, but for reaction dynamics in general. Mode-specific reaction for chemically bound systems has not been widely observed, mainly because randomization of energy among the internal modes of a molecule occurs before reaction can take place, even if the energy is initially placed into a specific local mode.

The results of this study show that CH_2NNO_2 exhibits nonstatistical, mode-specific behavior when certain normal modes of vibration are excited. There is substantial enhancement of the rates for both Reactions [1] and [2] as well as changes in branching ratios upon excitations of certain modes. We provide a simple analysis to show why the mode-specific reactions occur.

2. POTENTIAL ENERGY SURFACE

The analytic form, parameters values, and a description of features of the PES are given in Rice et al. (to be published). Reactant and transition state structures predicted by the model PES agree with the ab initio structures to within 0.5%. Also, the normal modes of vibration for the reactant and transition state species predicted by the model PES are in good agreement with the ab initio predictions (Mowrey et al. 1990). Additionally, the PES was fitted to points along the reaction path for Reaction [2] calculated by Mowrey et al. (1990). The model PES predicts an activation energy of 31.8 kcal/mol, in good agreement with the Mowrey et al. estimate. The dissociation energy of the N-N bond in the model was fixed at 35 kcal/mol, the value determined by Mowrey et al. (1990). Figures 1 and 2 show, respectively, the eigenvectors of the normal modes of vibration, predicted by the ab initio (Mowrey 1990) calculations and by the analytic PES used in this study.

3. METHODS

Classical trajectories were integrated using a variable-step size Adams-Moulton fourth-order predictor-corrector integrator (Miller and George 1972), with error tolerance set to 10^{-7} . The trajectories were integrated in a lab-fixed cartesian coordinate frame.

The energy of the system for each ensemble described below is 57.7 kcal/mol above the zero-point energy of the molecule (27.5 kcal/mol), for a total of 85.2 kcal/mol. Two methods were used to select initial conditions.

The first is Metropolis Monte Carlo (Metropolis et al. 1953) selection of initial conditions, with the angular momentum restricted (Viswanathan, Raff, and Thompson 1985) to zero. This selection ensures that energy will be partitioned statistically among the vibrational modes of the molecule. A total of 2,000 trajectories, including trajectories recounted according to the standard Metropolis sampling procedure (Metropolis et al. 1953; Raff and Thompson 1985), were calculated. This ensemble will be denoted throughout this report as the reference set and is used for comparisons with the results of ensembles with mode-selective initial conditions. The angular momentum was restricted in the initial condition selections of this ensemble, because we want to make this calculation comparable to those in which normal modes are excited. Also, the maximum bond extensions were restricted to confine initial condition selection to

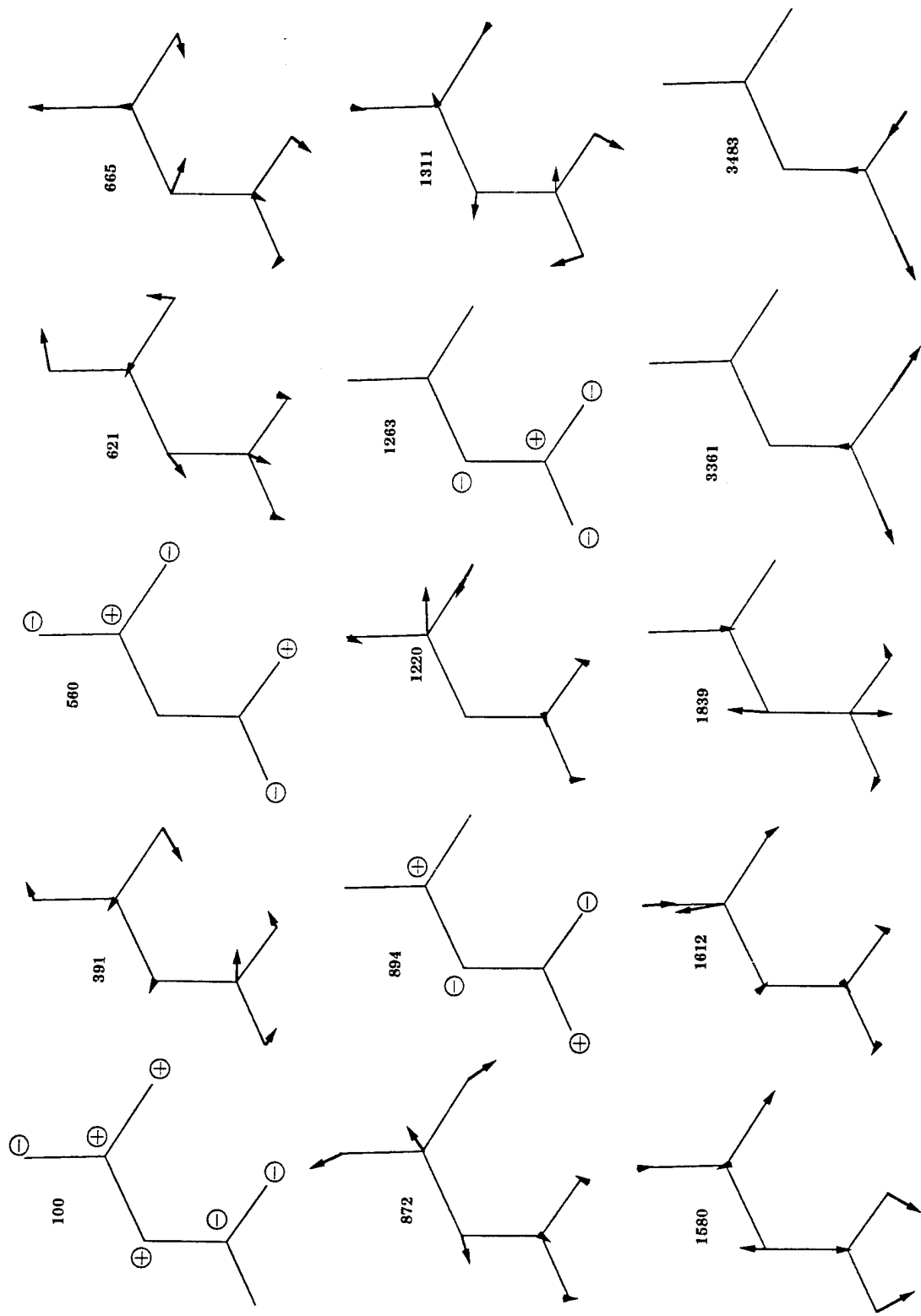


Figure 1. Depiction of the normal modes of vibration of equilibrium CH_2NNO_2 , predicted by Mowrey et al. (1990).

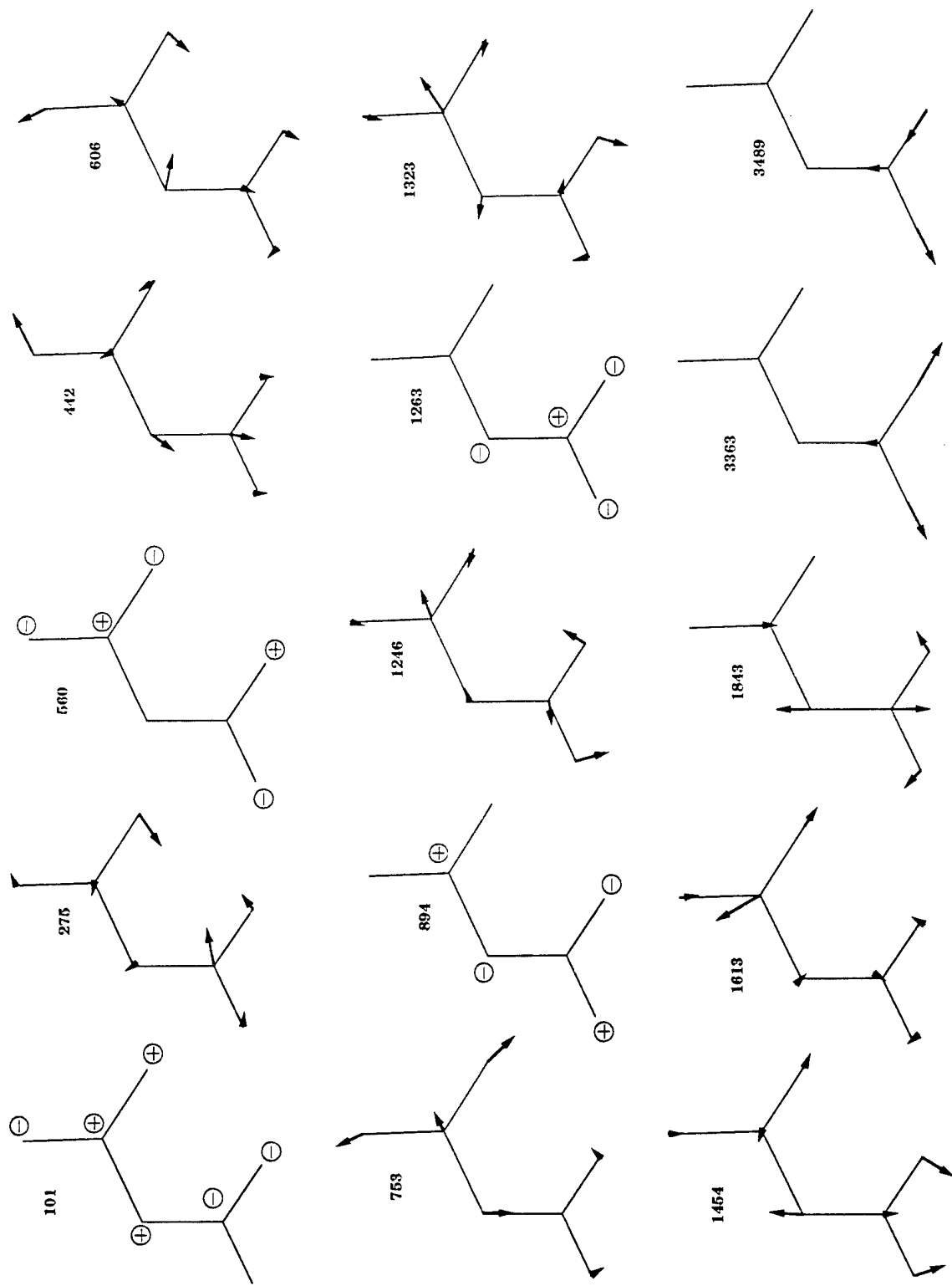


Figure 2. Depiction of the normal modes of vibration of equilibrium CH_2NNO_2 predicted by the analytic PES used in this study and in Zhao, Hintsa, and Lee 1988.

the reactant configuration space. The N-N and C-H bonds were limited to less than 2.0 and 1.2 Å, respectively, and the H-O bond was restricted to be greater than 1.6 Å.

The second method of initial condition selection involves first distributing zero-point energy among the normal modes of vibration, then placing 57.7 kcal/mol into one of the 15 normal modes of the molecule. The energy of each mode is partitioned according to a randomly-selected phase of the vibration from the appropriate distribution (Raff and Thompson 1985; Bintz 1986). Once the vibrational phase is selected, the difference in the energy calculated in the normal mode approximation and the potential energy using the model PES is determined and added in the form of kinetic energy to the vibrational modes. Occasionally, the potential energy calculated with the model PES exceeds the harmonic normal mode energy. In these cases, the initial conditions were rejected. Additionally, initial conditions were rejected if they violated the restrictions on bond extensions, as described in the previous paragraph. Each ensemble with initial conditions selected in this manner consisted of at least 1,000 trajectories. At least 2,000 trajectories were included in the ensembles that showed nonstatistical (i.e., nonlinear) behavior in the decay curves, to make certain the features were reproducible. The different ensembles will be referred to by the vibrational frequency (in cm^{-1}) of the normal mode that is initially excited to 57.7 kcal/mol above the zero-point energy.

Trajectories for both types of initial conditions were integrated until conditions specified in Table 1 were met. When the end-tests specifying HONO formation, Reaction [2], were satisfied, a second set of end-tests were triggered and the trajectory was continued until the second set of end-tests (for secondary reaction of HONO) were satisfied or until 20 ps total integration time elapsed.

The overall decay rate for a system that decomposes through two competing paths can be expressed as:

$$k_{\text{Total}} = k_1 + K_2. \quad (1)$$

k_{Total} can be obtained by the fitting of trajectory results to

$$\ln[P] = k_{\text{Total}}t, \quad (2)$$

where [P] is the fraction of unreacted CH_2NNO_2 at time t . The individual rate coefficients k_1 and K_2 are equal to the branching ratio

Table 1. End Tests

Primary Decomposition Reactions
$\text{CH}_2\text{NNO}_2 \rightarrow \text{H}_2\text{CN} + \text{NO}_2$ $R_{\text{NN}} > 5.0 \text{ \AA}, R_{\text{CH}(1)} < 2.0 \text{ \AA}, R_{\text{CH}(2)} < 2.0 \text{ \AA}$
$\text{CH}_2\text{NNO}_2 \rightarrow \text{HONO}' + \text{'HCN}$ $R_{\text{CH}} > 2.0 \text{ \AA}, R_{\text{OH}} < 1.393 \text{ \AA}, R_{\text{CH}'} < 2.0 \text{ \AA}$ and $D_{\text{NN}}, D_{\text{CH}} < 10^{-4} \text{ eV}$
Secondary Decomposition/Isomerization Reactions
$\text{HONO}' \rightarrow \text{H} + \text{ONO}'$ $R_{\text{RO}} > 5.0 \text{ \AA}$
$\text{HONO}' \rightarrow \text{ONO}'\text{H}$ $R_{\text{HO}} > R_{\text{HO}'}$
$\text{HONO}' \rightarrow \text{HO} + \text{NO}'$ $R_{\text{NO}} > 5.0 \text{ \AA}, R_{\text{NO}'} < 2.0 \text{ \AA}$

$$k_1 / k_2 = N_1 / N_2, \quad (3)$$

where N_i is the number of products for Reaction i , $i=1$ or 2 . The ratio N_1 / N_2 is computed as a function of time.

4. RESULTS AND DISCUSSION

We have used classical trajectories to investigate mode selectivity in CH_2NNO_2 . We calculated decay curves for initial conditions corresponding to excitation of each of the 15 normal modes. For comparison, we calculated one ensemble with the total energy distributed randomly among all the vibrational modes.

The computed decay curves are shown in Figure 3 for the 16 sets of initial conditions. The plot in Figure 3a is for the statistical initial conditions obtained by using Metropolis sampling. The remaining plots [frames (b)–(p)] in Figure 3 are for initial conditions corresponding to excitations of 57.7 kcal/mol of each of the 15 normal modes; the plots are arranged in order of increasing frequency of the excited mode.

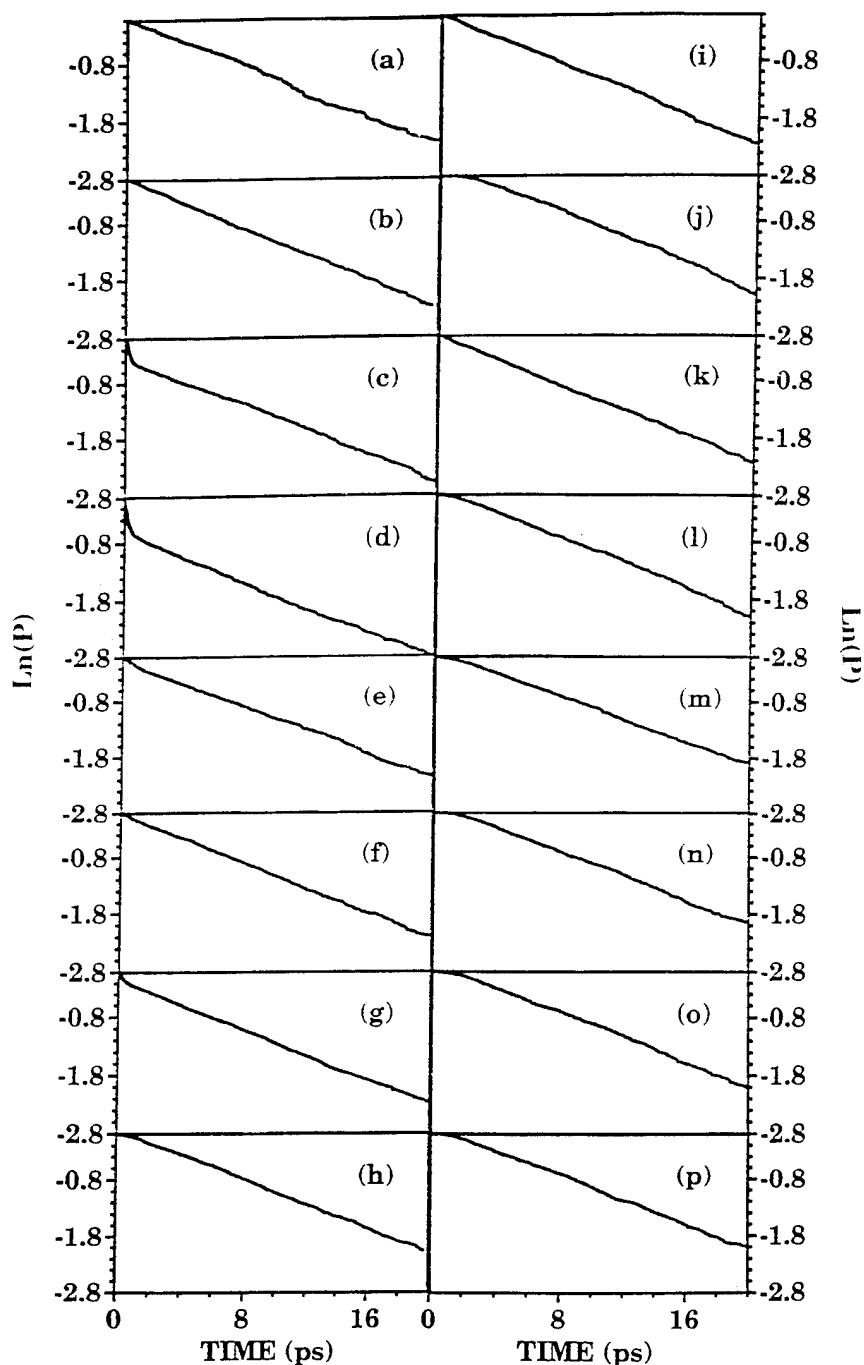


Figure 3. Decay curves for (a) Reference set (statistical initial conditions); (b) Mode 101; (c) Mode 275; (d) Mode 442; (e) Mode 560; (f) Mode 606; (g) Mode 753; (h) Mode 894; (i) Mode 1246; (j) Mode 1263, (k) Mode 1323; (l) Mode 1454; (m) Mode 1613; (n) Mode 1843; (o) Mode 3363; and (p) Mode 3489. The results are for total energy of zero-point energy plus 57.7 kcal/mol excitation with zero angular momentum. All of the plots show simple first-order decay except for those in frames (c), (d), and (g), which consist of two linear regions.

All but three [frames (c), (d), and (g)] of the plots in Figure 3 are linear over the time period (20 ps) of the trajectory integrations. The three nonlinear plots consist of two linear regions. There are "fast" and "slow" portions in these curves. The "fast" portion of the curves occurs between 0.0 and 0.4–0.5 ps for Figures 3c, 3d, and 3g. These are trajectories for which Modes 275, 442, and 753 were excited to 57.7 kcal/mol above the zero-point energy. We fitted Equations (2) and (3) to both the "fast" and "slow" portions of the curves in Figures 3c, 3d, and 3g and extracted rate coefficients for each region.

Plots of the branching ratios [see Equation (3)] are shown in Figures 4 and 5. The results shown in Figure 4 are for those ensembles with mode selected initial conditions that give linear decay curves (see Figure 3). Figure 5 shows the branching ratio plots for the "reference" ensemble with an initial random distribution of energy [frame (a)] and for the ensembles that yield nonlinear decay curves. The latter (Figures 5b–d) are also nonlinear, as expected.

The results of the fits for each set of decay and branching ratio curves are shown in Table 2. Additionally, we have illustrated the rate coefficients k_{Total} , k_1 , and k_2 in Figure 6 as functions of initial condition selection. The label "Reference" denotes initial conditions selected with angular-momentum restricted metropolis sampling (Raff and Thompson 1985; Miller and George 1972), and the frequency labels denote the mode that is excited above the zero-point energy. For those three modes that have two linear regions in the decay curves (Modes 275, 442, and 753), we have used the rate coefficients extracted from the "slow" portion of the decay curve. k_{Total} in this figure is $0.11 \pm 0.01 \text{ ps}^{-1}$; k_1 and k_2 are 0.07 and $0.04 \pm 0.01 \text{ ps}^{-1}$, respectively.

The agreement of the mode-selected results for modes that have a single linear decay curve with the reference set indicates that the decay rates are statistical. Also, the slow portion of the curves that have two linear regions predict the same rate coefficients as the results that show statistical behavior.

The rate coefficients calculated from the fast portion of the Mode 275 curve, shown in Table 2, indicate that Reactions [1] and [2] are substantially enhanced, with HONO formation favored slightly. The rates for Reactions [1] and [2] are also enhanced when Mode 442 is excited, but the effect is most pronounced for Reaction [1]. Excitation of Mode 753 causes some enhancement of the rates for Reactions [1] and [2] but not to the degree upon excitation of Modes 275 and 442.

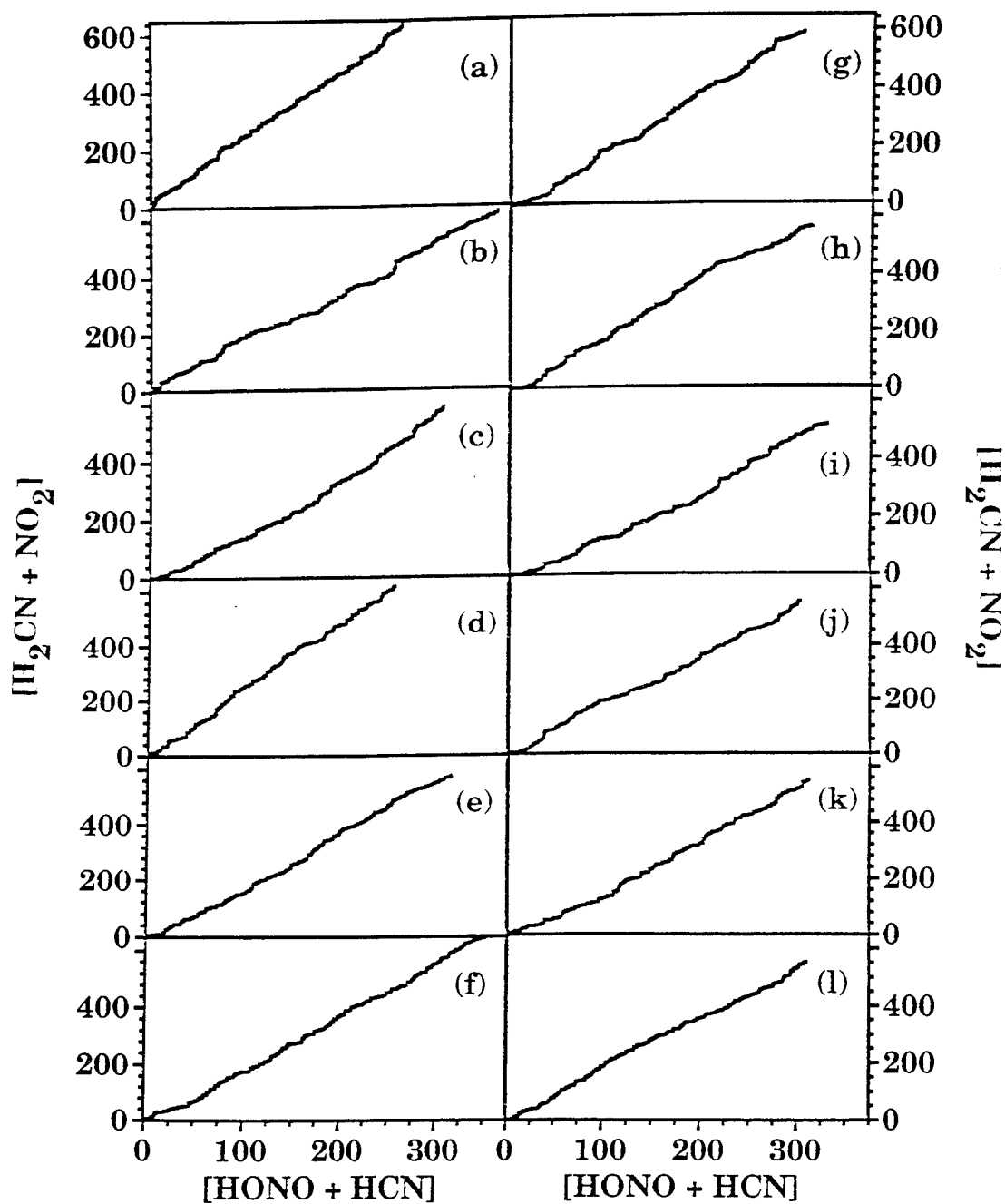


Figure 4. Branching ratios for (a) Mode 101; (b) Mode 560; (c) Mode 606; (d) Mode 894; (e) Mode 1246; (f) Mode 1263; (g) Mode 1323; (h) Mode 1454; (i) Mode 1613; (j) Mode 1843; (k) Mode 3363; and (l) Mode 3489. These linear plots correspond to the linear decay curves shown in Figure 3. The branching ratios for the nonlinear decay curves (Figures 3a, 3d, and 3g) are shown in Figure 5.

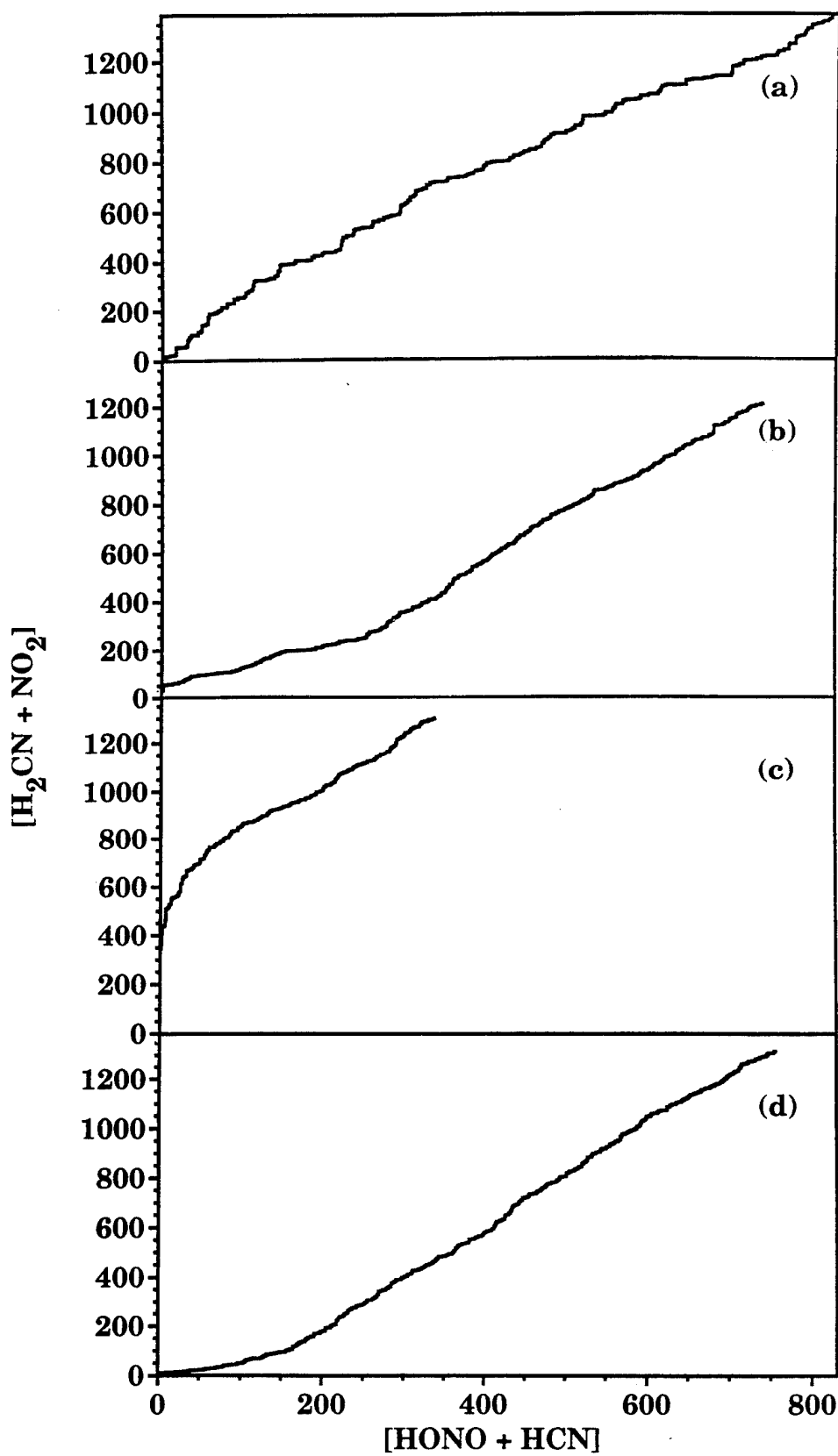


Figure 5. Branching ratios for (a) Reference set; (b) Mode 275; (c) Mode 442; and (d) Mode 753.

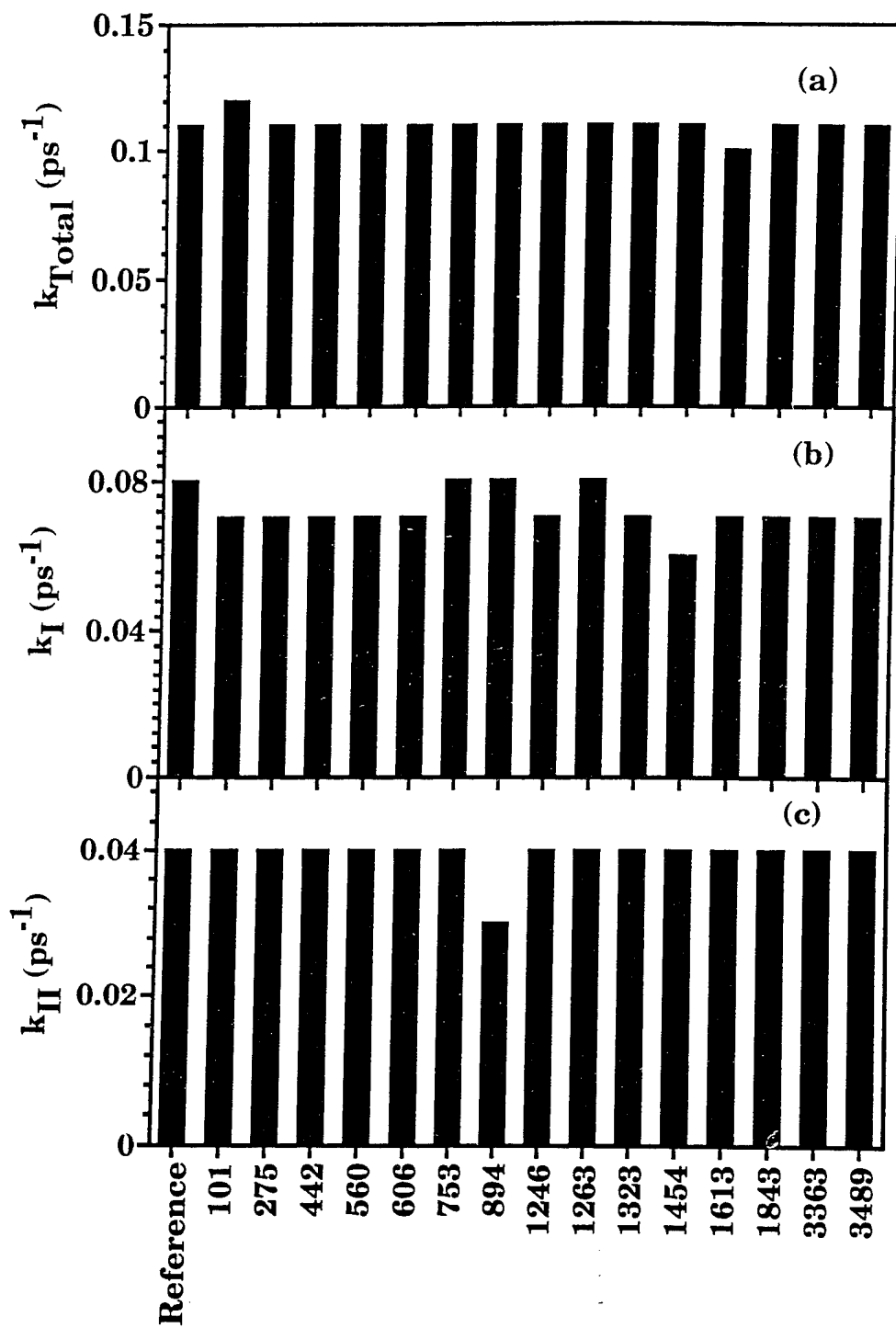


Figure 6. Comparison of (a) k_{Total} , (b) k_I , and (c) k_2 as a function of initial condition selection. The Reference refers to the angular-momentum-restricted Metropolis sampled ensemble, and the remaining values along the abscissa refer to the normal mode of vibration that is excited above the zero-point energy.

Table 2. Decay Coefficients and Branching Ratios

Ensemble	k_{Total} (ps^{-1})	k_1 (ps^{-1})	k_2 (ps^{-1})	k_1 / k_2
Reference	0.11	0.07	0.04	1.6
101	0.12	0.55	0.04	2.3
275 (fast)	1.13	0.07	0.59	0.9
(slow)	0.11	1.18	0.04	1.9
442 (fast)	1.29	0.07	0.11	11.3
(slow)	0.11	0.07	0.04	1.9
560	0.11	0.07	0.04	1.7
606	0.11	0.18	0.04	1.9
753 (fast)	0.40	0.07	0.22	0.8
(slow)	0.11	0.08	0.04	2.1
894	0.11	0.08	0.03	2.4
1246	0.11	0.07	0.04	1.9
1263	0.11	0.08	0.04	1.9
1323	0.11	0.07	0.04	2.1
1454	0.11	0.06	0.04	1.9
1613	0.10	0.07	0.04	1.7
1843	0.11	0.07	0.04	1.8
3363	0.11	0.07	0.04	1.8
3489	0.11	0.07	0.04	1.8

Ensemble averages and statistical information are listed in Table 3. Substantial fractions of trajectories in the ensembles contribute to the fast portion of the decay curves. Approximately 33%, 45%, and 18% of the total number of trajectories for the ensembles corresponding to Modes 275, 442, and 753, respectively, react within the time of the "fast" portion of the decay curves.

Why do these particular modes exhibit selective behavior in the reactions and the others do not? The answer is not evidence from a simple inspection of the normal modes. For example, based on inspection of the normal mode eigenvectors, one might predict that excitation of Mode 275 might increase the rate of Reaction [2] since its motion appears to be related to the Reaction [1]. However, this same simple inspection would not lead one to conclude that excitation of Mode 753 would show enhancement. Furthermore, based only on the normal mode representations shown in Figure 1, one might predict that excitations of Modes 606, 1246, and perhaps 1323 would show enhancement of Reaction [2]. Clearly, such a simple method of analysis by inspection is insufficient.

Table 3. Ensemble Results: Primary Decomposition Reactions

Ensemble ^a	Total Trajectories	Total Reactions	Total Reaction [1]	Total Reaction [2] ^a
Reference	2,505	2,215	1,388	827 (23)
101	1,000	897	635	262 (2)
275 (fast, 0.0–0.4 ps)	616	616	346	270 (4)
(slow, 0.4–20. ps)	1,496	1,333	861	472 (39)
442 (fast, 0.0–0.5 ps)	793	793	737	56 (0)
(slow, 0.5–20. ps)	954	847	564	283 (6)
560	1,122	993	630	363 (8)
606	1,000	890	583	307 (8)
753 (fast, 0.0–0.5 ps)	370	370	177	193 (0)
(slow, 0.5–20. ps)	1,945	1,706	1,141	565 (14)
894	1,000	873	616	257 (6)
1246	1,000	893	576	317 (4)
1263	1,141	1,001	648	353 (5)
1323	1,000	893	589	304 (3)
1454	1,000	878	565	313 (9)
1613	1,000	848	517	331 (4)
1843	999	856	553	303 (4)
3363	1,000	866	553	313 (4)
3489	1,000	863	552	311 (5)

^aValues in parentheses are the number of trajectories resulting in secondary HONO decomposition.

Although the coupling between the selected mode and the reaction coordinate at the reactant equilibrium geometry is necessary, as assumed in the analysis by inspection of the normal modes discussed previously, mode specificity depends on the coupling well along the reaction coordinate (perhaps up to the transition state). And, of course, it also depends on the couplings of the selected mode to the "bath" modes, that is, those not associated with the reaction coordinate; these couplings determine the rate of energy randomization. Waite and Miller (1981) used this sort of analysis in a study of a model system (a Modified Henon-Heiles potential [Henon and Heiles 1964]).

We have determined the minimum energy paths for Reactions [1] and [2] using the definition given by Miller, Handy, and Adams (1980). These are shown in Figures 7 and 8. The reaction path is defined as the path of steepest descent from the saddle point toward reactant or product. Because Reaction [1] has no saddle point, but rather a barrier equal to the reaction endothermicity, we used the approximation of large N-N separation to begin the steepest descents (see Rai and Truhlar [1983]). The reaction paths were calculated using the POLYRATE 5.0.1 set of computer codes (Lu et al. 1992; Liu et al. 1993).

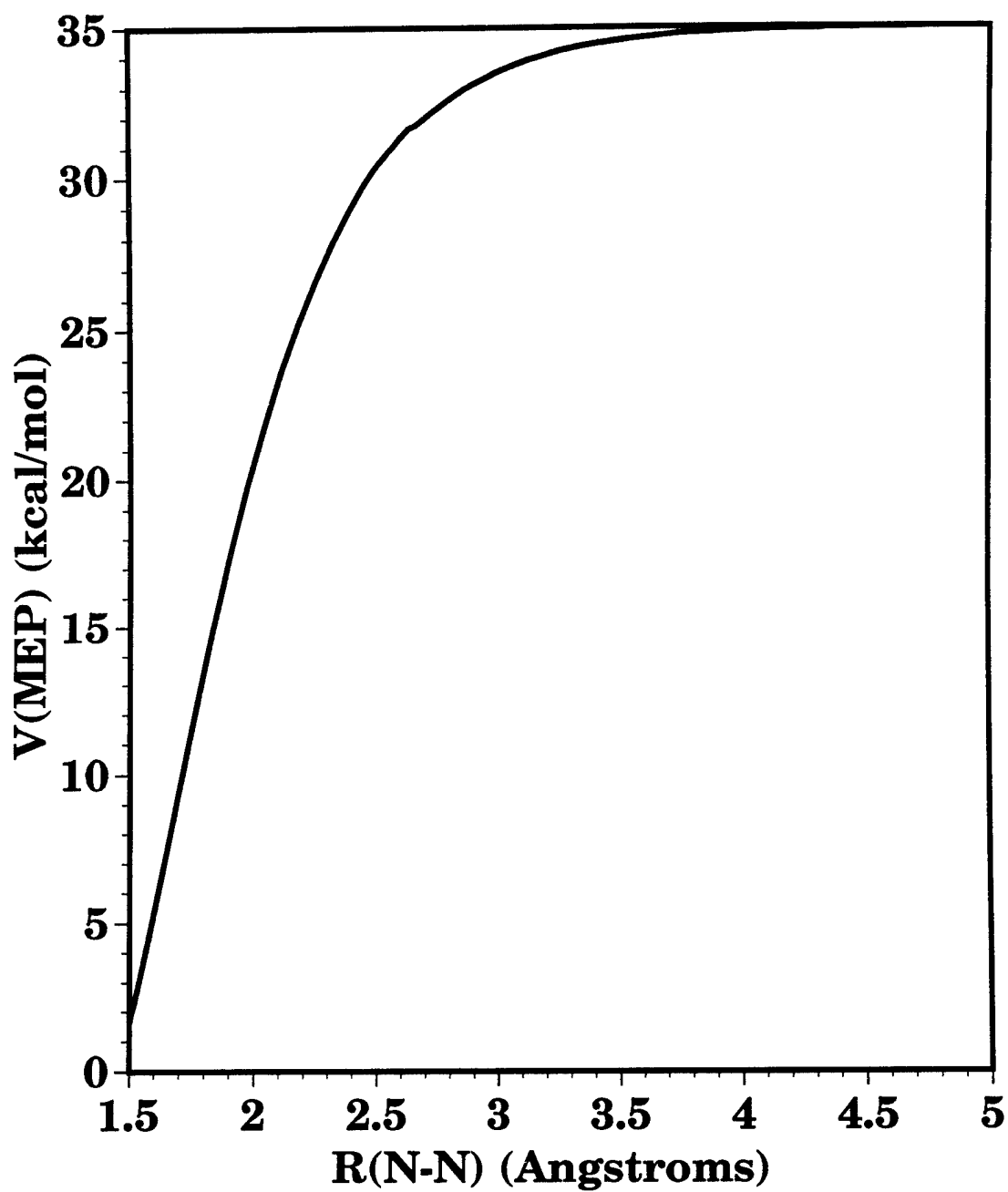


Figure 7. Potential energy along the reaction path for Reaction [1]. The MEP path for Reaction [1] has no barrier to the back reaction as is typical for simple bond rupture reactions.

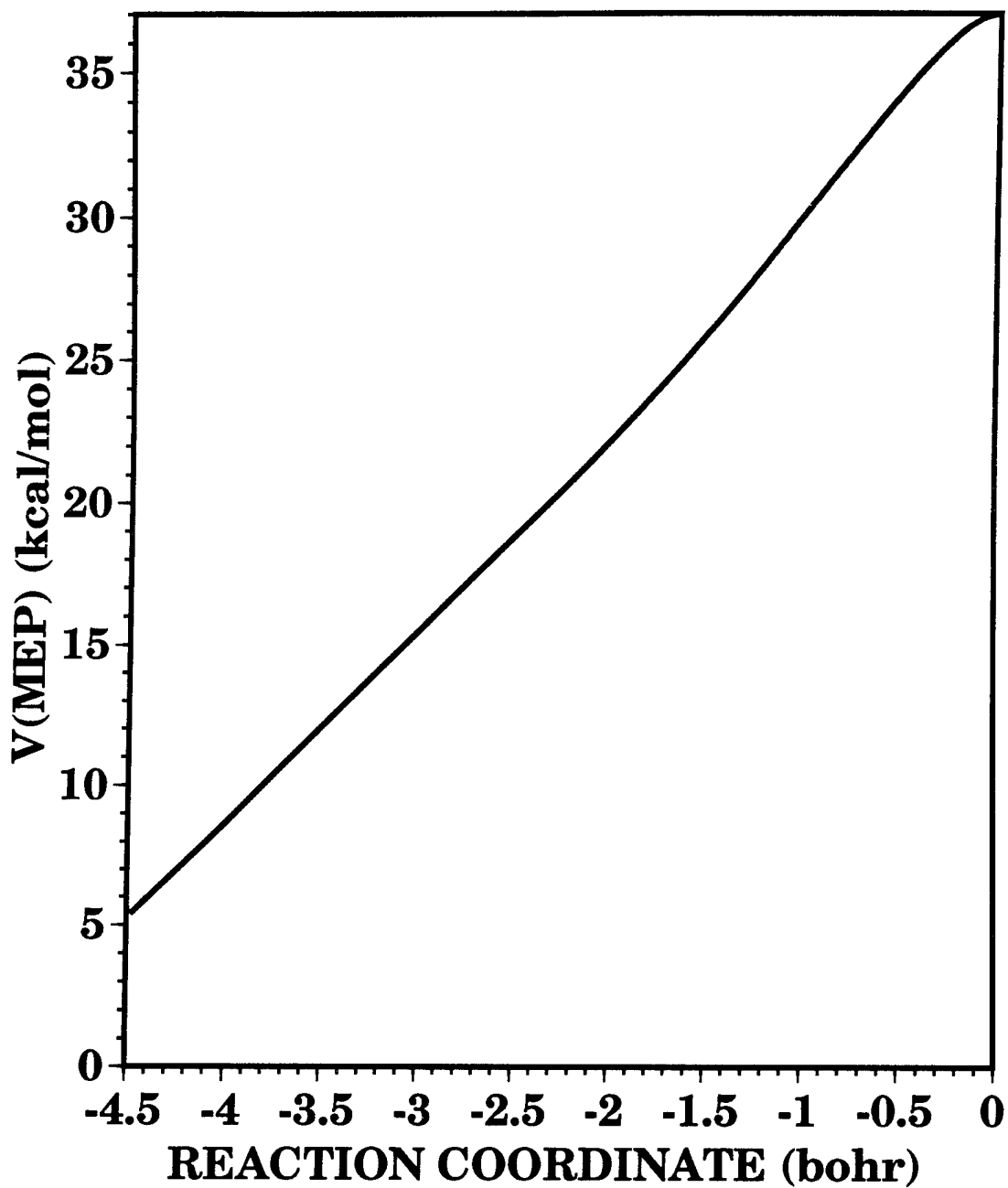


Figure 8. Potential energy along the reaction path for Reaction [2]. The equilibrium CH_2NNO_2 is located at $-4.5 a_0$, and the saddle point is located at $0.0 a_0$.

To determine the extent of the coupling of each vibrational mode of CH_2NNO_2 with the two reaction coordinates, we projected its eigenvector onto the eigenvectors for points all along the reaction path that correspond to the direction along the reaction path, as defined in Miller, Handy, and Adams 1980. The results of the projections of the normal modes of vibration onto the reaction paths of Reactions [1] and [2] are shown in Figure 9. Figure 9a shows the projection of the vibrational modes onto the reaction path for Reaction [1]; clearly Modes 275, 442, and 753 have the largest projections onto the path for N-N distances less than 2.5 Å. For N-N distances greater than 2.5 Å, the projection of vibrational Mode 275 is small while the projections of Modes 442 and 753 remain large. The other modes do not strongly project into this reaction coordinate.

Figure 9b shows the projection of the vibrational modes onto the reaction path for Reaction [2]. The value of $s = -4.5 a_0$ is near equilibrium CH_2NNO_2 and $s = 0.0 a_0$ corresponds to the saddle point for Reaction [2]. For s in the range -4.5 to $-2.5 a_0$, only Modes 442, 753, and 606 show substantial coupling with the reaction coordinate. For s greater than $-2.5 a_0$, Modes 275 and 606 project most strongly onto this reaction path. If Mode 606 did not project onto the coordinate for Reaction [2], we would conclude that projection of a vibrational motion on the reaction coordinate is not only necessary, as shown by Waite and Miller (1981), but sufficient to show mode-specific chemistry for this system. However, excitation of Mode 606 does not give mode-specific reaction. The decay curve for this mode and the resulting rate coefficients are in good agreement with the result for the statistical reference set. Why does this vibrational mode show no mode specificity when it clearly projects onto the reaction coordinate for Reaction [2]? It is because mode-specific dynamics depend on the rate of energy randomization vs. the rate of the chemical process.

To investigate this, we monitored the normal mode energies for the first 0.1–0.25 ps for 50 trajectories randomly selected from each of the ensembles in which the 275, 442, 606, and 753 modes were initially excited (Figures 10–13, respectively). Figure 10 shows the results for the ensemble in which Mode 275 is excited; energy rapidly transfers out of this mode into many other modes, including Modes 753 and 442. The total average harmonic energy quickly exceeds the actual energy calculated using the model PES, indicating that the normal mode approximation at this level of excitation is poor. However, this representation of energy flow with respect to vibrational motion is the simplest way to follow the energy changes due to those motions in a system of this complexity. Note that motion corresponding to Mode 606 receives little excitation.

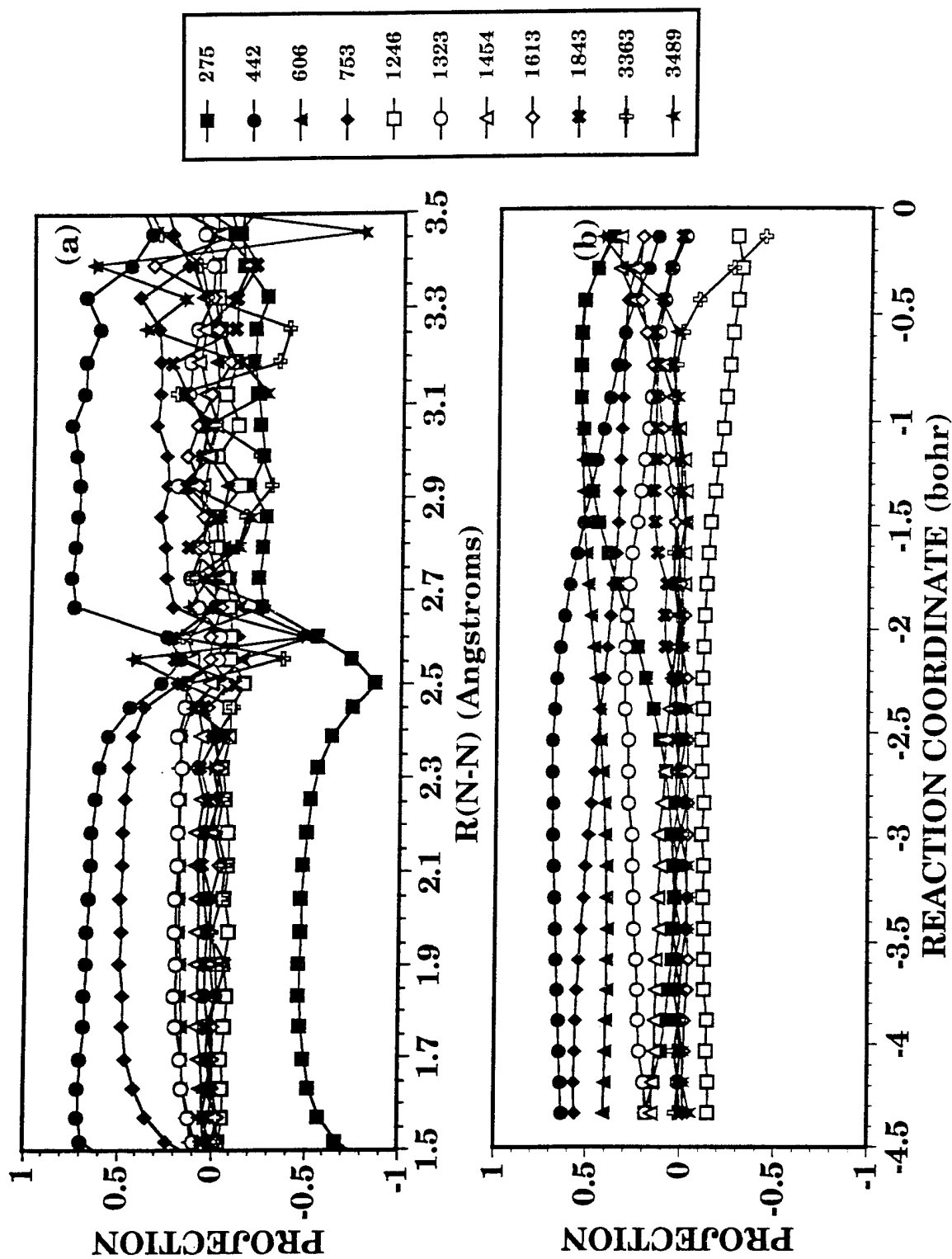


Figure 9. Projection of the eigenvectors of the normal modes of CH_2NNO_2 (at equilibrium) onto the unit vector that points along the reaction path for (a) Reaction [1] and (b) Reaction [2]. The unit vector corresponding to the direction along the reaction path is calculated at various points along the reaction coordinate for the two reactions.

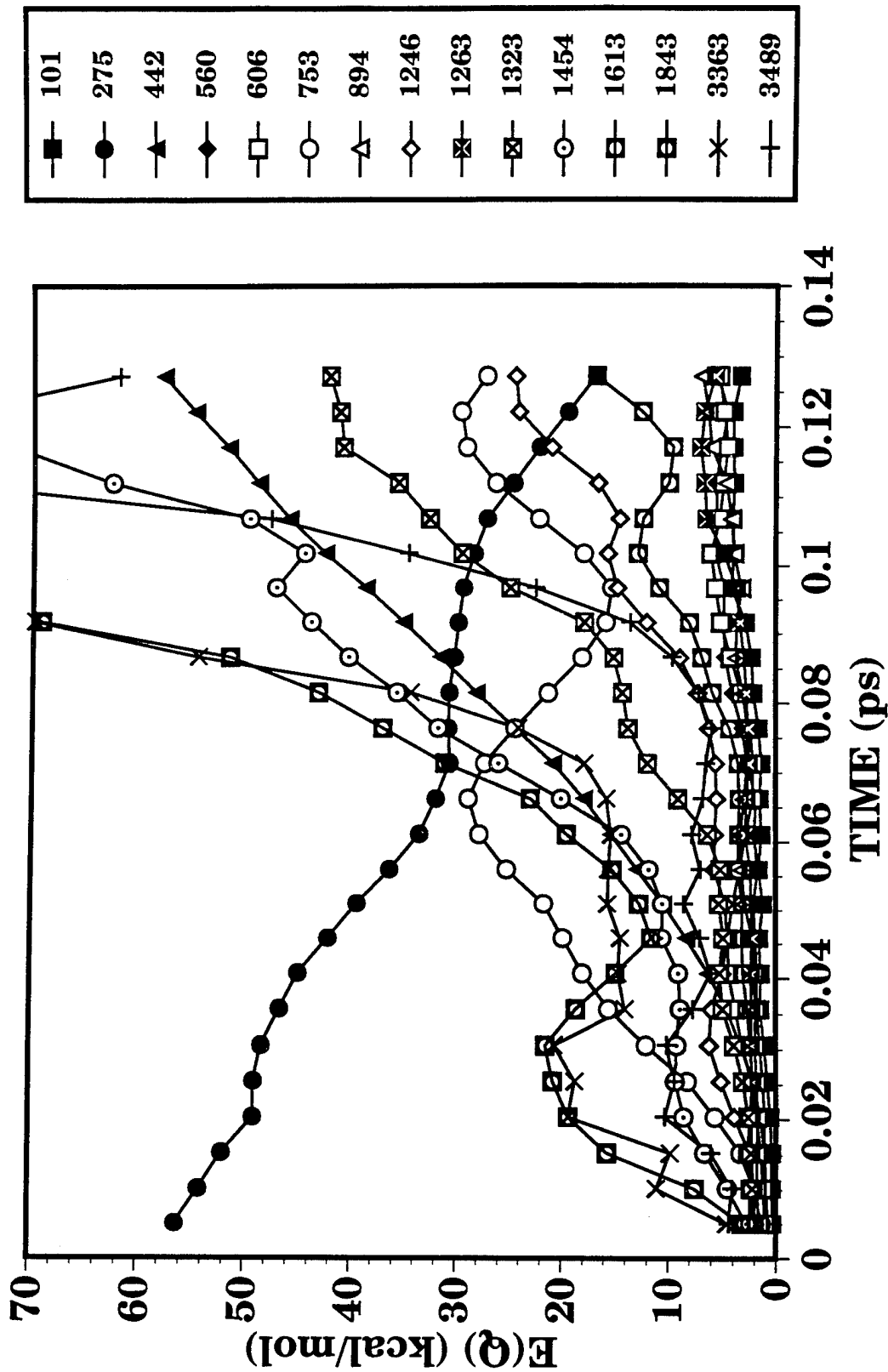


Figure 10. Normal mode energy vs. time averaged over 50 trajectories for which 57.7 kcal/mol was initially placed in Mode 275. The legend denotes the normal mode by its frequency in cm^{-1} .

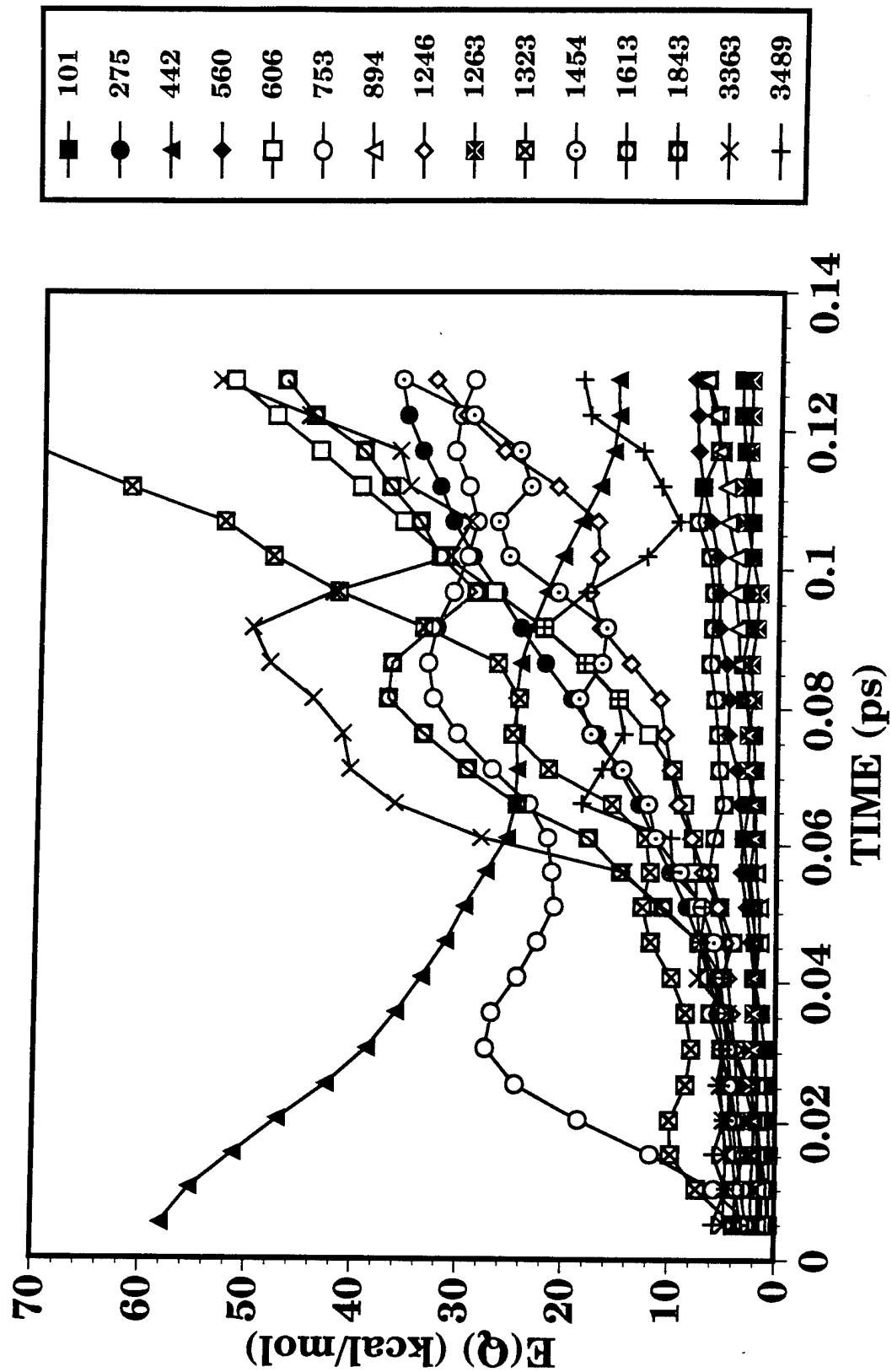


Figure 11. Normal mode energy vs. time averaged over 50 trajectories for which 57.7 kcal/mol was initially placed in Mode 442. The legend denotes the normal mode by its frequency in cm^{-1} .

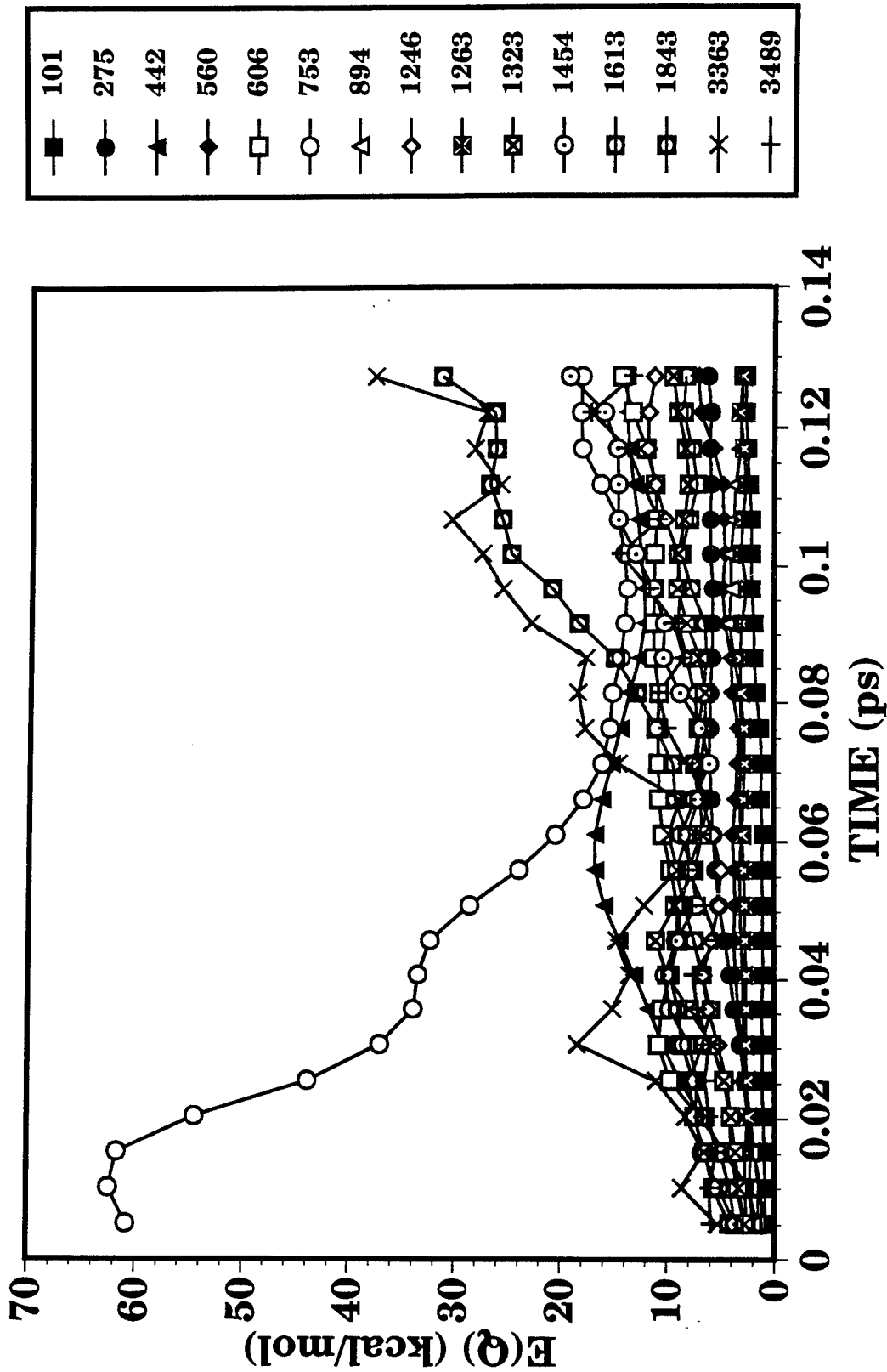


Figure 12. Normal mode energy vs. time averaged over 50 trajectories for which 57.7 kcal/mol was initially placed in Mode 753. The legend denotes the normal mode by its frequency in cm^{-1} .

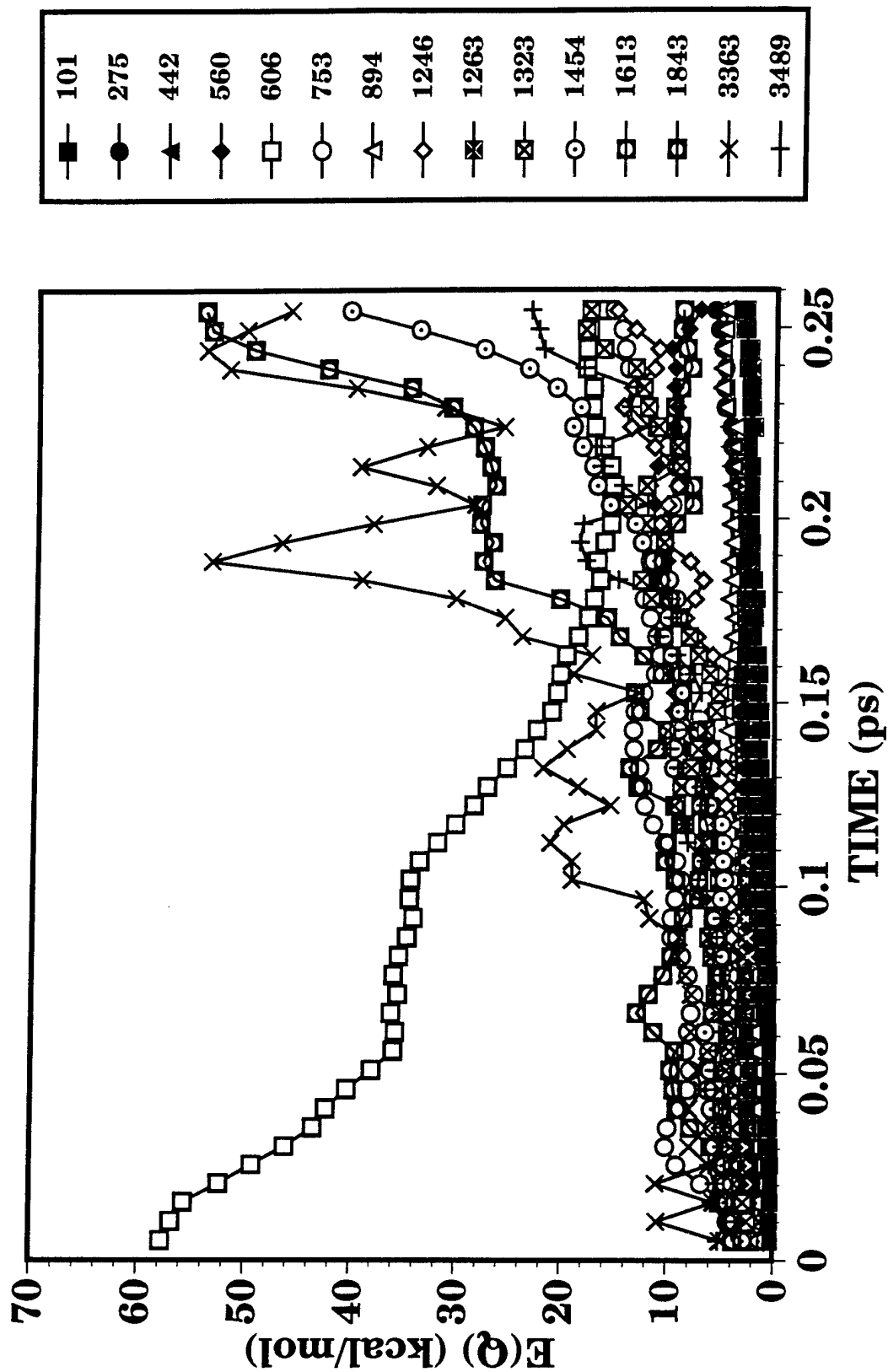


Figure 13. Normal mode energy vs. time averaged over 50 trajectories for which 57.7 kcal/mol was initially placed in Mode 606. The legend denotes the normal mode by its frequency in cm^{-1} .

Figure 11, which shows the average normal mode energies for 50 trajectories randomly selected from the mode-excited 442 ensemble, is similar to Figure 10; energy rapidly transfers from Mode 442, first to 753 and then to many other modes, including Mode 275. In this case, Mode 606 is excited along with many of the other vibrations. Figure 12 shows the results of averaged normal mode energies for trajectories selected from the ensemble of mode-excited 753; energy rapidly transfers from this mode, mainly into Modes 442, 3363, and 1613. Mode 275 does not receive much of the energy. The reaction rate for this ensemble shows the least enhancement of the three ensembles that exhibit mode-specific reaction.

Figure 13, which shows the average normal mode energies for trajectories from mode-excited 606, is substantially different from Figures 10–12 over the same time interval. Fewer modes become excited due to energy transfer out of Mode 606. We followed the energy transfer twice as long as for the other modes to see if the energy would randomize among all the modes, as seen in the other cases. The modes that receive the most energy are 3363, 1613, and 1454. None of these vibrational modes show mode-specific effects in the decomposition dynamics. Note that in this ensemble, modes corresponding to the motions that yield enhanced reaction, 275, 442, and 753, show little, if any, excitation due to the energy transfer.

The trajectory results and this simple analysis using the projection of the vibrational modes onto the reaction coordinates show that while vibrational coupling to the reaction coordinate is necessary to cause mode-specific behavior, the energy for reaction must remain trapped among modes coupled to the reaction coordinates rather than leak out to modes that are not coupled to the reaction coordinates. This clearly is the case with Mode 606, which shows strong projection onto the path for Reaction [2] yet transfers energy into modes that are not coupled into the reaction coordinate. It would appear that the energy transfer into these "bath" modes is faster than energy transfer to the reaction coordinate. On the other hand, the modes that exhibit specificity are both coupled to the reaction coordinates and at least one of the other "coupled" vibrational modes (modes with frequencies 275, 442, and 753 cm^{-1}). This suggests that the energy necessary for reaction is "trapped" among modes that couple strongly with the reaction coordinate long enough for the energy to flow into a reaction coordinate leading to the increased reaction rate.

We also investigated combinations of mode excitations to determine if they further enhance the rates. Partitioning the excitation energy equally into pairs of modes that did not exhibit mode-specific behavior

did not change the decomposition dynamics; the decay curves appeared linear with the same slope as the statistical ensemble. We put 28.85 kcal/mol into each of Modes 275 and 442 (for a total of 57.7 kcal/mol) and calculated an ensemble of approximately 2,500 trajectories. The resulting decay and branching ratio curves are shown in Figures 14 and 15. The fast portion of the decay curve (shown along with the linear fit of Equation (2) in the inset of Figure 14) occurs over the range 0.0–0.15 ps. The slope of the slow portion of the decay curve matches the statistical (reference) ensemble result. One-third of the reactions occur by 0.15 ps. The fit of Equation (2) to the fast portion of the decay curve predicts that the rate for Reaction [2] is increased by 6,700% above the statistical rate, and Reaction [2] is favored over Reaction [1] by a factor of 4.6. The rate for Reaction [1] is increased by 750% above the statistical value, and is similar to the result when Mode 275 is singularly excited.

5. SUMMARY

We have presented the results of classical trajectory calculations of the unimolecular decomposition of CH_2NNO_2 for mode-selective initial conditions. The two primary decomposition pathways of this molecule are (I) simple scission of the N-N bond to form H_2CN and NO_2 and (II) concerted dissociation via a five-centered transition state to form HONO and HCN. Fifteen ensembles of 1,000 to 2,500 trajectories, each corresponding to a specific vibrational mode excited to 57.7 kcal/mol above the zero-point energy, provided decay curves and branching ratios, from which rate coefficients were determined. Three of the decay curves, corresponding to ensembles of trajectories in which modes with frequencies 275, 442, and 753 cm^{-1} were excited to 57.7 kcal/mol, showed two regions of linear behavior. The curves are similar in that the portions of the decay curves with a steeper slope (denoted the fast region) ranged from 0 to 0.5 ps and the portions of the curves with the more gradual slope (the slow region) resembled the result for random initial conditions. The fast region of the curves showed that rates for Reactions [1] and [2] are increased, with the most dramatic enhancement occurring for excitation of the modes with frequencies 275 and 442 cm^{-1} (see Figures 1 and 2 for definitions of the normal modes). Trajectories corresponding to excitation of the normal mode with frequency 275 cm^{-1} shows almost equally enhanced rates for Reactions [1] and [2], while the rate of Reaction [1] is increased by over an order of magnitude upon excitation of the normal mode with frequency 442 cm^{-1} . Although excitation of the mode with frequency 753 cm^{-1} leads to an increased rate, the effect is not nearly as dramatic as for the modes with frequencies 275 and 442 cm^{-1} . Decay curves and branching ratios obtained from ensembles of trajectories corresponding to excitation of one of each of the remaining 12 vibrational modes are linear, and agree with the results for random initial conditions.

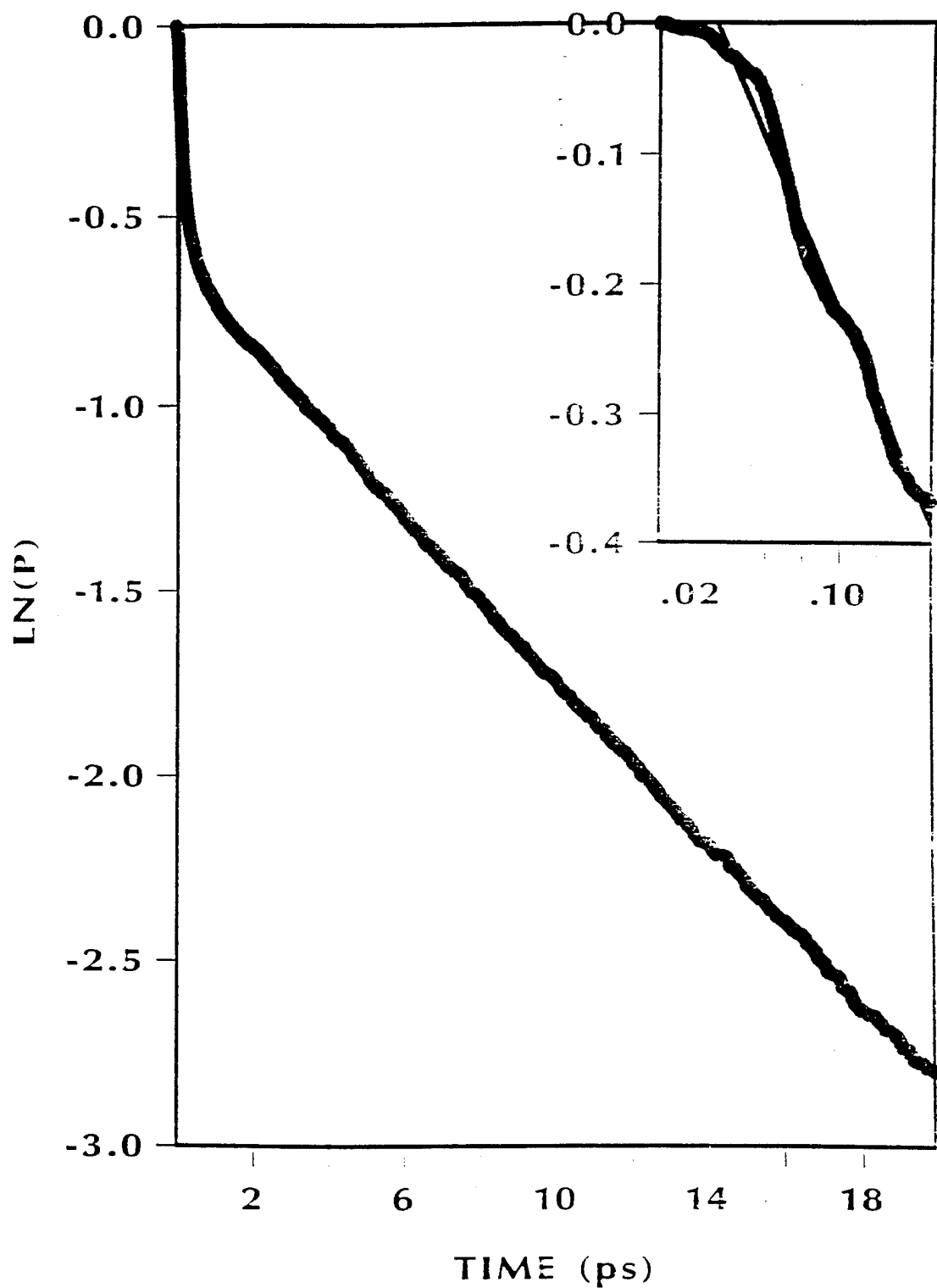


Figure 14. Decay curve for trajectory ensemble in which 57.7 kcal/mol above the zero-point energy is equally partitioned to Modes 275 and 442. The inset shows the region of the decay curve from 0.0 – 0.15 ps, and the fit of this region to equation (2). Approximately one-third of all reactions occur within this time range under these initial conditions.

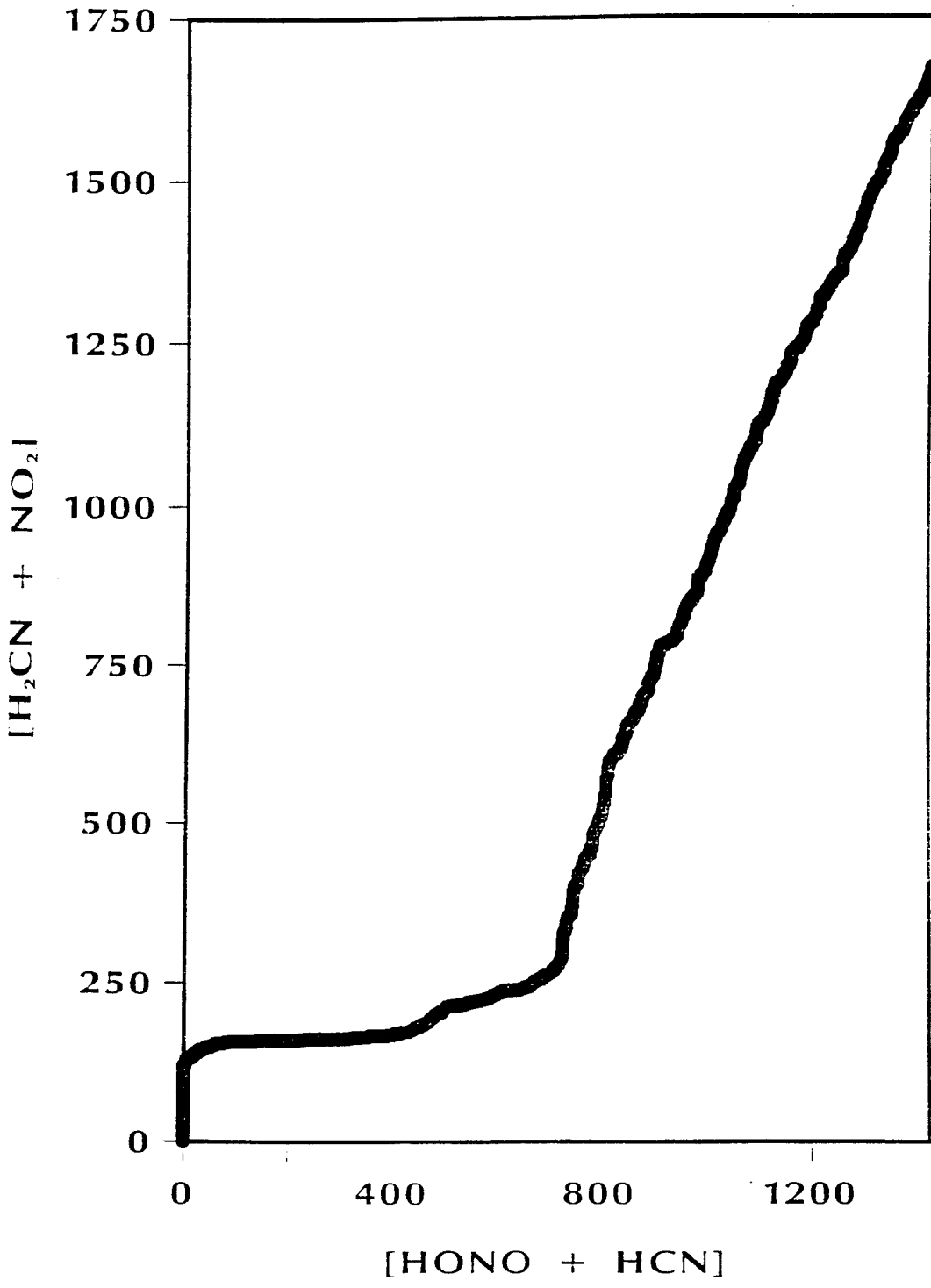


Figure 15. Branching ratios corresponding to the decay curve shown in Figure 14.

The basis of the mode specificity is illustrated by projecting the eigenvectors of the normal modes of vibration of CH_2NNO_2 onto the reaction paths for Reactions [1] and [2]. The modes that exhibit selectivity in the reactions project strongly onto the two reaction paths. An additional vibrational mode (frequency 606 cm^{-1}) also projects strongly onto the path for Reaction [2] but shows no enhancement of the rate. Our results indicate that energy transfers out of the mode with frequency 606 cm^{-1} into vibrational modes that are not coupled to the reaction coordinates more quickly than it flows into the reaction coordinates. The modes with frequencies 275 , 442 , and 753 cm^{-1} are coupled among themselves, and as energy transfers out of one of these, it flows into other mode(s) that project onto the reaction coordinates. In other words, the energy is trapped in modes that are strongly coupled to the reaction coordinates.

In addition to confirming conditions necessary for mode-specific reaction, we have given credence to the possibility that upon formation of CH_2NNO_2 through the decomposition of RDX, reaction energy is placed preferentially into the reaction coordinate for Reaction [2] or into vibrational modes that are strongly coupled to the reaction coordinate for Reaction [2]. This could explain why concerted reaction is singularly observed (Zhao, Hintsa, and Lee 1988) at the expense of the simpler bond-rupture reaction.

INTENTIONALLY LEFT BLANK.

6. REFERENCES

- Bintz, K. L. Master's Thesis. Oklahoma State University, OK, 1986.
- Henon, M., and C. Heiles. Astron. J., vol. 69, p. 73, 1964.
- Liu, Y. -P., G. C. Lynch, W. -P. Hu, V. S. Melissas, R. Steckler, B. C. Garrett, D. -H. Lu, T. N. Truong, A. D. Isaacson, S. N. Rai, G. C. Hancock, J. G. Lauderdale, T. Joseph, and D. G. Truhlar, POLYRATE, QCPE Program 601-version 5.0.1; Quantum Chemistry Program Exchange, Indiana University, Bloomington, IN, 1993; QCPE Bulletin, vol. 13, pp. 28-29, 1993.
- Lu, D. -H., T. N. Truong, V. S. Melissas, G. C. Lynch, Y. -P. Liu, B. C. Garrett, R. Steckler, A. D. Isaacson, S. N. Rai, G. C. Hancock, J. G. Lauderdale, T. Joseph, and D. G. Truhlar, Computer Physics Communications, vol., 71, p. 235, 1992.
- Metropolis, N., A. W. Rosenbluth, M. N. Rosenbluth, A. H. Teller, and E. Teller. Journal of Chemical Physics, vol. 21, p. 1087, 1953.
- Miller, W. H., N. C. Handy, and J. E. Adams. Journal of Chemical Physics, vol. 72, p. 99, 1980.
- Miller, W. H., and T. F. George. Journal of Chemical Physics, vol. 56, p. 5668, 1972.
- Mowrey R. C., M. Page, G. F. Adams, and B. H. Lengsfeld, III. Journal of Chemical Physics, vol. 93, p. 1857, 1990.
- Raff, L. M., and D. L. Thompson. Theory of Chemical Reaction Dynamics, vol. 4, edited by M. Baer, (Boca Raton, FL: CRC Press, 1985).
- Rai, S. N., and D. G. Truhlar. Journal of Chemical Physics, vol. 79, p. 6046, 1983.
- Rice, B. M., G. F. Adams, M. Page, and D. L. Thompson. Journal of Physical Chemistry, to be published.
- Robinson, P. J., and K. A. Holbrook. Unimolecular Reactions. New York: Wiley, 1972.
- Viswanathan, R., L. M. Raff, and D. L. Thompson. Journal of Chemical Physics, vol. 82, p. 3083, 1985.
- Waite, B. A., and W. H. Miller. Journal of Chemical Physics, vol. 74, p. 3910, 1981.
- Zhao, X., E. J. Hints, and Y. T. Lee. Journal of Chemical Physics, vol. 88, p. 801, 1988.

INTENTIONALLY LEFT BLANK.

NO. OF
COPIES ORGANIZATION

2 ADMINISTRATOR
ATTN DTIC DDA
DEFENSE TECHNICAL INFO CTR
CAMERON STATION
ALEXANDRIA VA 22304-6145

1 DIRECTOR
ATTN AMSRL OP SD TA
US ARMY RESEARCH LAB
2800 POWDER MILL RD
ADELPHI MD 20783-1145

3 DIRECTOR
ATTN AMSRL OP SD TL
US ARMY RESEARCH LAB
2800 POWDER MILL RD
ADELPHI MD 20783-1145

1 DIRECTOR
ATTN AMSRL OP SD TP
US ARMY RESEARCH LAB
2800 POWDER MILL RD
ADELPHI MD 20783-1145

ABERDEEN PROVING GROUND

5 DIR USARL
ATTN AMSRL OP AP L (305)

<u>NO. OF COPIES</u>	<u>ORGANIZATION</u>
1	HQDA ATTN SARD TR MS K KOMINOS PENTAGON WASHINGTON DC 20310-0103
1	HQDA ATTN SARD TR DR R CHAIT PENTAGON WASHINGTON DC 20310-0103
1	HQDA OASA RDA ATTN DR C H CHURCH PENTAGON ROOM 3E486 WASHINGTON DC 20310-0103
4	COMMANDER ATTN R GHIRARDELLI D MANN R SINGLETON R SHAW US ARMY RESEARCH OFFICE P O BOX 12211 RSCH TRNGLE PK NC 27709-2211
1	DIRECTOR ATTN AMXRO MCS K CLARK ARMY RESEARCH OFFICE P O BOX 12211 RSCH TRNGLE PK NC 27709-2211
1	DIRECTOR ATTN AMXRO RT IP LIB SERVICES ARMY RESEARCH OFFICE P O BOX 12211 RSCH TRNGLE PK NC 27709-2211
2	COMMANDER ATTN SMCAR AEE B D S DOWNS US ARMY ARDEC PCTNY ARSNL NJ 07806-5000
2	COMMANDER ATTN SMCAR AEE J A LANNON US ARMY ARDEC PCTNY ARSNL NJ 07806-5000
1	COMMANDER ATTN SMCAR AEE BR L HARRIS US ARMY ARDEC PCTNY ARSNL NJ 07806-5000

<u>NO. OF COPIES</u>	<u>ORGANIZATION</u>
2	COMMANDER ATTN AMSMI RD PR E A R MAYKUT AMSMI RD PR P R BETTS US ARMY MISSILE COMMAND REDSTONE ARSENAL AL
1	OFFICE OF NAVAL RESEARCH DEPARTMENT OF THE NAVY ATTN R S MILLER CODE 432 800 N QUINCY STREET ARLINGTON VA 22217
1	COMMANDER ATTN J RAMNARACE AIR 54111C NAVAL AIR SYSTEMS COMMAND WASHINGTON DC 20360
2	COMMANDER ATTN R BERNECKER R 13 G B WILMOT R 16 NAVAL SURFACE WARFARE CENTER SILVER SPRING MD 20903-5000
5	COMMANDER ATTN M C LIN J MCDONALD E ORAN J SHNUR R J DOYLE CODE 6110 NAVAL RESEARCH LABORATORY WASHINGTON DC 20375
2	COMMANDER ATTN T BOGGS CODE 388 T PARR CODE 3895 NAVAL WEAPONS CENTER CHINA LAKE CA 93555-6001
1	SUPERINTENDENT ATTN D W NETZER DEPT OF AERONAUTICS NAVAL POSTGRADUATE SCHOOL MONTEREY CA 93940
3	AL LSCF ATTN R CORLEY R GEISLER J LEVINE EDWARDS AFB CA 93523-5000

<u>NO. OF COPIES</u>	<u>ORGANIZATION</u>	<u>NO. OF COPIES</u>	<u>ORGANIZATION</u>
1	AFOSR ATTN J M TISHKOFF BOLLING AIR FORCE BASE WASHINGTON DC 20332	2	PRINCETON COMBUSTION RESEARCH LABORATORIES INC ATTN N A MESSINA M SUMMERFIELD PRINCETON CORPORATE PLAZA BLDG IV SUITE 119 11 DEERPARK DRIVE MONMOUTH JUNCTION NJ 08852
1	OSD SDIO IST ATTN L CAVENY PENTAGON WASHINGTON DC 20301-7100	3	DIRECTOR DIVISION 8354 ATTN S JOHNSTON P MATTERN D STEPHENSON SANDIA NATIONAL LABORATORIES LIVERMORE CA 94550
1	COMMANDANT ATTN ATSF TSM CN USAFAS FORT SILL OK 73503-5600	1	BRIGHAM YOUNG UNIVERSITY ATTN M W BECKSTEAD DEPT OF CHEMICAL ENGINEERING PROVO UT 84058
1	UNIV OF DAYTON RSCH INSTITUTE ATTN D CAMPBELL AL PAP EDWARDS AFB CA 93523	1	CALIFORNIA INSTITUTE OF TECH JET PROPULSION LABORATORY ATTN L STRAND MS 125 224 4800 OAK GROVE DRIVE PASADENA CA 91109
1	NASA ATTN G B NORTHAM MS 168 LANGLEY RESEARCH CENTER LANGLEY STATION HAMPTON VA 23365	1	CALIFORNIA INSTITUTE OF TECHNOLOGY ATTN F E C CULICK MC 301 46 204 KARMAN LAB PASADENA CA 91125
4	NATIONAL BUREAU OF STANDARDS ATTN J HASTIE M JACOX T KASHIWAGI H SEMERJIAN US DEPARTMENT OF COMMERCE WASHINGTON DC 20234	1	UNIVERSITY OF CALIFORNIA LOS ALAMOS SCIENTIFIC LAB P O BOX 1663 MAIL STOP B216 LOS ALAMOS NM 87545
2	DIRECTOR ATTN C WESTBROOK W TAO MS L 282 LAWRENCE LIVERMORE NATIONAL LAB P O BOX 808 LIVERMORE CA 94550	1	UNIVERSITY OF CALIFORNIA BERKELEY CHEMISTRY DEPARTMENT ATTN C BRADLEY MOORE 211 LEWIS HALL BERKELEY CA 94720
1	DIRECTOR ATTN B NICHOLS T7 MS B284 LOS ALAMOS NATIONAL LAB P O BOX 1663 LOS ALAMOS NM 87545	1	UNIVERSITY OF CALIFORNIA SAN DIEGO ATTN F A WILLIAMS AMES B010 LA JOLLA CA 92093
1	NATIONAL SCIENCE FOUNDATION ATTN A B HARVEY WASHINGTON DC 20550		

<u>NO. OF COPIES</u>	<u>ORGANIZATION</u>
2	UNIV OF CALIFORNIA SANTA BARBARA QUANTUM INSTITUTE ATTN K SCHOFIELD M STEINBERG SANTA BARBARA CA 93106
1	UNIV OF COLORADO AT BOULDER ENGINEERING CENTER ATTN J DAILY CAMPUS BOX 427 BOULDER CO 80309-0427
3	UNIV OF SOUTHERN CALIFORNIA DEPT OF CHEMISTRY ATTN R BEAUDET S BENSON C WITTIG LOS ANGELES CA 90007
1	CORNELL UNIVERSITY DEPARTMENT OF CHEMISTRY ATTN T A COOL BAKER LABORATORY ITHACA NY 14853
1	UNIVERSITY OF DELAWARE ATTN T BRILL CHEMISTRY DEPARTMENT NEWARK DE 19711
1	UNIVERSITY OF FLORIDA ATTN J WINEFORDNER DEPT OF CHEMISTRY GAINESVILLE FL 32611
3	GEORGIA INSTITUTE OF TECHNOLOGY SCHOOL OF AEROSPACE ENGINEERING ATTN E PRICE W C STRAHLE B T ZINN ATLANTA GA 30332
1	UNIVERSITY OF ILLINOIS DEPT OF MECH ENG ATTN H KRIER 144MEB 1206 W GREEN ST URBANA IL 61801
1	THE JOHNS HOPKINS UNIV CPIA ATTN T W CHRISTIAN 10630 LITTLE PATUXENT PKWY SUITE 202 COLUMBIA MD 21044-3200

<u>NO. OF COPIES</u>	<u>ORGANIZATION</u>
1	UNIVERSITY OF MICHIGAN GAS DYNAMICS LAB ATTN G M FAETH AEROSPACE ENGINEERING BLDG ANN ARBOR MI 48109-2140
1	UNIVERSITY OF MINNESOTA DEPT OF MECHANICAL ENGINEERING ATTN E FLETCHER MINNEAPOLIS MN 55455
4	PENNSYLVANIA STATE UNIVERSITY DEPT OF MECHANICAL ENGINEERING ATTN K KUO M MICCI S THYNELL V YANG UNIVERSITY PARK PA 16802
1	POLYTECHNIC INSTITUTE OF NY GRADUATE CENTER ATTN S LEDERMAN ROUTE 110 FARMINGDALE NY 11735
2	PRINCETON UNIVERSITY FORRESTAL CAMPUS LIBRARY ATTN K BREZINSKY I GLASSMAN P O BOX 710 PRINCETON NJ 08540
1	PURDUE UNIVERSITY SCHOOL OF AERONAUTICS AND ASTRONAUTICS ATTN J R OSBORN GRISSOM HALL WEST LAFAYETTE IN 47906
1	PURDUE UNIVERSITY DEPARTMENT OF CHEMISTRY ATTN E GRANT WEST LAFAYETTE IN 47906
2	PURDUE UNIVERSITY SCHOOL OF MECHANICAL ENGINEERING ATTN N M LAURENDEAU S N B MURTHY TSPC CHAFFEE HALL WEST LAFAYETTE IN 47906

<u>NO. OF COPIES</u>	<u>ORGANIZATION</u>	<u>NO. OF COPIES</u>	<u>ORGANIZATION</u>
1	RENSSELAER POLYTECHNIC INST DEPT OF CHEMICAL ENGINEERING ATTN A FONTIJN TROY NY 12181	1	EXXON RESEARCH & ENG CO ATTN A DEAN ROUTE 22E ANNANDALE NJ 08801
1	STANFORD UNIVERSITY DEPT OF MECHANICAL ENGINEERING ATTN R HANSON STANFORD CA 94305	1	GENERAL APPLIED SCIENCE LABS INC 77 RAYNOR AVENUE RONKONKAMA NY 11779-6649
1	UNIVERSITY OF TEXAS DEPT OF CHEMISTRY ATTN W GARDINER AUSTIN TX 78712	1	GENERAL ELECTRIC ORDNANCE SYSTEMS ATTN J MANDZY 100 PLASTICS AVENUE PITTSFIELD MA 01203
1	VA POLYTECH INST AND STATE UNIV ATTN J A SCHETZ BLACKSBURG VA 24061	1	GENERAL MOTORS RSCH LABS PHYSICAL CHEMISTRY DEPARTMENT ATTN T SLOANE WARREN MI 48090-9055
1	APPLIED COMBUSTION TECHNOLOGY INC ATTN A M VARNEY P O BOX 607885 ORLANDO FL 32860	2	HERCULES INC ATTN W B WALKUP E A YOUNT P O BOX 210 ROCKET CENTER WV 26726
2	APPLIED MECHANICS REVIEWS ASME ATTN R E WHITE & A B WENZEL 345 E 47TH STREET NEW YORK NY 10017	1	HERCULES INC ATTN R V CARTWRIGHT 100 HOWARD BLVD KENVIL NJ 07847
1	ATLANTIC RESEARCH CORP ATTN R H W WAESCHE 7511 WELLINGTON ROAD GAINESVILLE VA 22065	1	ALLIANT TECHSYSTEMS INC MARINE SYSTEMS GROUP ATTN D E BRODEN MS MN50 2000 600 2ND STREET NE HOPKINS MN 55343
1	TEXTRON DEFENSE SYSTEMS ATTN A PATRICK 2385 REVERE BEACH PARKWAY EVERETT MA 02149-5900	1	ALLIANT TECHSYSTEMS INC ATTN R E TOMPKINS MN 11 2720 600 SECOND ST NORTH HOPKINS MN 55343
1	BATTELLE TWSTIAC 505 KING AVENUE COLUMBUS OH 43201-2693	1	IBM CORPORATION ATTN A C TAM RESEARCH DIVISION 5600 COTTLE ROAD SAN JOSE CA 95193
1	COHEN PROFESSIONAL SERVICES ATTN N S COHEN 141 CHANNING STREET REDLANDS CA 92373	1	IIT RESEARCH INSTITUTE ATTN R F REMALY 10 WEST 35TH STREET CHICAGO IL 60616

<u>NO. OF COPIES</u>	<u>ORGANIZATION</u>
1	LOCKHEED MISSILES & SPACE CO ATTN GEORGE LO 3251 HANOVER STREET DEPT 52 35 B204 2 PALO ALTO CA 94304
1	OLIN ORDNANCE ATTN V MCDONALD LIBRARY P O BOX 222 ST MARKS FL 32355-0222
1	PAUL GOUGH ASSOCIATES INC ATTN P S GOUGH 1048 SOUTH STREET PORTSMOUTH NH 03801-5423
1	HUGHES AIRCRAFT COMPANY ATTN T E WARD 8433 FALLBROOK AVENUE CANOGA PARK CA 91303
1	ROCKWELL INTERNATIONAL CORP ROCKETDYNE DIVISION ATTN J E FLANAGAN HB02 6633 CANOGA AVENUE CANOGA PARK CA 91304
1	SCIENCE APPLICATIONS INC ATTN R B EDELMAN 23146 CUMORAH CREST WOODLAND HILLS CA 91364
3	SRI INTERNATIONAL ATTN G SMITH D CROSLEY D GOLDEN 333 RAVENSWOOD AVENUE MENLO PARK CA 94025
1	STEVENS INSTITUTE OF TECH DAVIDSON LABORATORY ATTN R MCALEVY III HOBOKEN NJ 07030
1	SVERDRUP TECHNOLOGY INC LERC GROUP ATTN R J LOCKE MS SVR 2 2001 AEROSPACE PARKWAY BROOK PARK OH 44142

<u>NO. OF COPIES</u>	<u>ORGANIZATION</u>
1	SVERDRUP TECHNOLOGY INC ATTN J DEUR 2001 AEROSPACE PARKWAY BROOK PARK OH 44142
3	THIOKOL CORPORATION ELKTON DIVISION ATTN R BIDDLE R WILLER TECH LIB P O BOX 241 ELKTON MD 21921
3	THIOKOL CORPORATION WASATCH DIVISION ATTN S J BENNETT P O BOX 524 BRIGHAM CITY UT 84302
1	UNITED TECHNOLOGIES RSCH CENTER ATTN A C ECKBRETH EAST HARTFORD CT 06108
1	UNITED TECHNOLOGIES CORP CHEMICAL SYSTEMS DIVISION ATTN R R MILLER P O BOX 49028 SAN JOSE CA 95161-9028
1	UNIVERSAL PROPULSION COMPANY ATTN H J MCSPADDEN 25401 NORTH CENTRAL AVENUE PHOENIX AZ 85027-7837
1	VERITAY TECHNOLOGY INC ATTN E B FISHER 4845 MILLERSPORT HIGHWAY EAST AMHERST NY 14051-0305
1	FREEDMAN ASSOCIATES ATTN E FREEDMAN 2411 DIANA ROAD BALTIMORE MD 21209-1525
1	ALLIANT TECHSYSTEMS ATTN J BODE 600 SECOND ST NE HOPKINS MN 55343

<u>NO. OF</u> <u>COPIES</u>	<u>ORGANIZATION</u>
1	ALLIANT TECHSYSTEMS ATTN C CANDLAND 600 SECOND ST NE HOPKINS MN 55343
1	ALLIANT TECHSYSTEMS ATTN L OSGOOD 600 SECOND ST NE HOPKINS MN 55343
1	ALLIANT TECHSYSTEMS ATTN R BURETTA 600 SECOND ST NE HOPKINS MN 55343
1	ALLIANT TECHSYSTEMS ATTN R BECKER 600 SECOND ST NE HOPKINS MN 55343
1	ALLIANT TECHSYSTEMS ATTN M SWENSON 600 SECOND ST NE HOPKINS MN 55343
1	US ARMY BENET LABORATORY ATTN SAM SOPOK SMCAR CCB B WATERVLIET NY 12189

<u>NO. OF</u> <u>COPIES</u>	<u>ORGANIZATION</u>
	<u>ABERDEEN PROVING GROUND</u>
36	DIR USARL ATTN: AMSRL-WT-P, A HORST AMSRL-WT-PC, R A FIFER G F ADAMS W R ANDERSON R A BEYER S W BUNTE C F CHABALOWSKI K P MC-NEILL BOONSTOPPEL A COHEN R CUMPTON R DANIEL D DEVYNCK N F FELL B E FORCH J M HEIMERL A J KOTLAR M R MANAA W F MCBRATNEY K L MCNESBY S V MEDLIN M S MILLER A W MIZIOLEK S H MODIANO J B MORRIS J E NEWBERRY S A NEWTON R A PESCE-RODRIGUEZ B M RICE R C SAUSA M A SCHROEDER J A VANDERHOFF M WENSING A WHREN J M WIDDER C WILLIAMSON AMSRL-CI-CA, R PATEL

INTENTIONALLY LEFT BLANK.

USER EVALUATION SHEET/CHANGE OF ADDRESS

This Laboratory undertakes a continuing effort to improve the quality of the reports it publishes. Your comments/answers to the items/questions below will aid us in our efforts.

1. ARL Report Number ARL-TR-740 Date of Report May 1995

2. Date Report Received _____

3. Does this report satisfy a need? (Comment on purpose, related project, or other area of interest for which the report will be used.) _____

4. Specifically, how is the report being used? (Information source, design data, procedure, source of ideas, etc.) _____

5. Has the information in this report led to any quantitative savings as far as man-hours or dollars saved, operating costs avoided, or efficiencies achieved, etc? If so, please elaborate. _____

6. General Comments. What do you think should be changed to improve future reports? (Indicate changes to organization, technical content, format, etc.) _____

CURRENT ADDRESS

Organization

Name

Street or P.O. Box No.

City, State, Zip Code

7. If indicating a Change of Address or Address Correction, please provide the Current or Correct address above and the Old or Incorrect address below.

OLD ADDRESS

Organization

Name

Street or P.O. Box No.

City, State, Zip Code

(Remove this sheet, fold as indicated, tape closed, and mail.)
(DO NOT STAPLE)

DEPARTMENT OF THE ARMY

OFFICIAL BUSINESS

BUSINESS REPLY MAIL

FIRST CLASS PERMIT NO 0001, APG, MD

POSTAGE WILL BE PAID BY ADDRESSEE

DIRECTOR
U.S. ARMY RESEARCH LABORATORY
ATTN: AMSRL-WT-PC
ABERDEEN PROVING GROUND, MD 21005-5066



NO POSTAGE
NECESSARY
IF MAILED
IN THE
UNITED STATES

